European Journal of Pharmaceutics and Biopharmaceutics 139 (2019) 1–22

Contents lists available at ScienceDirect

European Journal of Pharmaceutics and Biopharmaceutics

journal homepage: www.elsevier.com/locate/ejpb

Review article

An overview of electrospun membranes loaded with bioactive molecules for improving the wound healing process

Sónia P. Miguel[a,1], Rosa S. Sequeira[a,1], André F. Moreira[a], Cátia S.D. Cabral[a], António G. Mendonça[a,b], Paula Ferreira[c], Ilídio J. Correia[a,c,*]

[a] CICS-UBI – Centro de Investigação em Ciências da Saúde, Universidade da Beira Interior, Av. Infante D. Henrique, 6200-506 Covilhã, Portugal
[b] Departamento de Química, Universidade da Beira Interior, R. Marquês d'Ávila e Bolama, 6201-001 Covilhã, Portugal
[c] CIEPQPF – Departamento de Engenharia Química, Universidade de Coimbra, Rua Silvio Lima, 3030-790 Coimbra, Portugal

ARTICLE INFO

Keywords:
Antimicrobial molecules
Biological molecules
Drug delivery systems
Electrospun nanofibers
Wound dressing

ABSTRACT

Nowadays, despite the intensive research performed in the area of skin tissue engineering, the treatment of skin lesions remains a big challenge for healthcare professionals. In fact, none of the wound dressings currently used in the clinic is capable of re-establishing all the native features of skin. An ideal wound dressing must confer protection to the wound from external microorganisms, chemical, and physical aggressions, as well as promote the healing process by stimulating the cell adhesion, differentiation, and proliferation. In recent years different types of wound dressings (such as films, hydrocolloids, hydrogels, micro/nano fibers) have been developed. Among them, electrospun nanofibrous membranes due to their intrinsic properties like high surface area-to-volume ratio, porosity and structural similarity with the skin extracellular matrix have been regarded as highly promising for wound dressings applications. Additionally, the nanofibers available in these membranes can act as drug delivery systems, which prompted the incorporation of biomolecules within their structure to prevent skin infections as well as improve the healing process. In this review, examples of different bioactive molecules that have been loaded on polymeric nanofibers are presented, highlighting the antibacterial biomolecules (*e.g.* antibiotics, silver nanoparticles and natural extracts-derived products) and the molecules capable of enhancing the healing process (*e.g.* growth factors, vitamins, and anti-inflammatory molecules).

1. Introduction

Since ancient times, the wound treatment procedure comprises the covering of the wound site with a dressing material that avoids patient dehydration and the occurrence of infections. The dressings used up to recent years acted as protective materials known as gauzes, bandages or cotton wool. Although, these dressings promoted the formation of scar tissue, in some cases they also induce a new lesion when replaced [1,2]. Nowadays, different types of wound dressings (such as films, hydrocolloids, hydrogels, and micro/nano fibers) have been developed to provide a moist environment as well as prompt cell adhesion and proliferation, in order to enhance the healing process [3]. Furthermore, such wound dressings are biodegradable, exhibit a non-toxic profile, allow the absorption of wound exudates, prevent patient dehydration, and circumvent the formation of eschar [2,4].

Wound dressings composed of electrospun nanofibers display auspicious properties for improving the healing process. Their 3D architecture mimics the structure of the skin extracellular matrix (ECM), which plays a pivotal role in supporting cell adhesion and proliferation [5–9]. Further, the porous structure of these matrices is compatible with the adsorption of wound exudates, gaseous and nutrients exchanges, as well as prevents bacterial invasion [10,11]. Besides, electrospun nanofibers can be functionalized with bioactive molecules that can enhance the wound healing [1,9,12]. In fact, the combination of the large surface area to volume ratio of the nanofibers with the possibility of selecting the most appropriate solvent for drug solubilization grant to these dressings high loading capacities [12–14]. Moreover, the drug loading in these devices can be performed using different methodologies that spawn from the biomolecules blending with the polymer to the incorporation of secondary drug carriers [15,16]. On the other hand, the biomolecules release can be specifically tailored to fulfill the demands of the different phases of the healing process, *i.e.* hemostasis, inflammation, migration, proliferation or remodelling [1,13,15]. Researchers have been incorporating different

* Corresponding author.
E-mail address: icorreia@ubi.pt (I.J. Correia).
[1] Authors contributed equally to this work.

https://doi.org/10.1016/j.ejpb.2019.03.010
Received 15 January 2019; Received in revised form 27 February 2019; Accepted 6 March 2019
Available online 07 March 2019

antibacterial and biological agents in nanofibers to improve their performance in the healing process [17,18]. The results obtained revealed that these dressings were able to avoid bacterial penetration (*e.g.* nanofibers functionalized with antibiotics, silver-based materials, and bactericidal natural compounds) or to enhance the wound healing (*e.g.* nanofibers incorporating growth factors (GFs), vitamins, and anti-inflammatory molecules) [10,15,19,20].

In this review, an overview of the most prominent biologic active molecules that have been, so far, incorporated into electrospun nanofibers aiming to prevent skin infections as well as improve/encourage the healing process is provided. In addition, future perspectives regarding the application of electrospun nanofibers based-drug delivery systems for improving skin tissue regeneration are also highlighted.

2. Electrospun membranes used as drug delivery systems

The optimization of different electrospinning parameters (*e.g.* the raw materials, viscosity, applied voltage, flow rate, temperature, humidity, etc) allows the production of the nanofibers with specific features, such as mean diameter, surface area/volume ratio, porosity, wettability, and mechanical properties [21–23]. Furthermore, the nanofibers drug loading can be performed using different methodologies that comprise the incorporation of the biologic active agents before the electrospinning process be performed, through co-axial, multi-jet, emulsion, and secondary carrier electrospinning [9,15,24]. Moreover, the nanofibers surface can also be modified by physical adsorption, layer-by-layer assembly and chemical immobilization of biomolecules (as illustrated in Fig. 1). An overview of these strategies was already been reviewed elsewhere [9,15,25]. By combining these strategies, researchers can control the encapsulation of multiple biomolecules. Depending on the role of a biomolecule in the healing process, the drug release profile can be tailored through the incorporation method used [26]. For example, the physical adsorption of biomolecules into nanofibers is frequently associated with burst releases and short diffusion times, whereas the co-axial electrospinning allows a more controlled and sustained release profile [27,28]. On the other hand, if the different molecules are incorporated into nanofibers by the same method, the drug release profile will be dependent on the diffusion coefficient of each molecule. In these cases, the rate of biomolecule diffusion out of the polymeric matrix will be affected by several factors like polymer swelling, polymer erosion, biomolecular dissolution/diffusion characteristics, biomolecules distribution inside the matrix and biomolecule/polymer ratio [16,29,30].

In the following sections, the loading of bioactive molecules into nanofibers in order to confer them additional antimicrobial properties, improve the biological performance of the membranes, and ultimately enhance the healing process will be discussed.

3. Biomolecules with antimicrobial activity that have been incorporated into electrospun membranes

After skin infections occur, microorganisms' invasion prompt the deterioration of the granulation tissue, GFs and ECM components (*e.g.* collagen, elastin, and fibrin), compromising the healing process [31,32]. Thus, in order to prevent such deleterious effects, it is imperative to use wound dressings that are able to prevent bacterial penetration into the wound as well as to support skin regeneration (as illustrated in Fig. 2). In the following topics, the different antimicrobial agents (*e.g.* antibiotics, silver nanoparticles (AgNPs) and natural extracts-derived products) that have been loaded into electrospun nanofibers for enhancing their antibacterial properties are overviewed.

3.1. Antibiotics

In the clinic antibiotics are widely used, mainly those administered through oral administration, for preventing/treating microbial colonization/contamination of open wounds. Nevertheless, this therapeutic approach presents several disadvantages such as rapid elimination from blood stream, degradation, and narrow therapeutic windows. In this way, to overcome these limitations, researchers have been exploring the topical administration of antibiotics through their incorporation in wound dressings. Ciprofloxacin (CIF), gentamycin, tetracycline, and silver sulfadiazine (SSD) have been incorporated into electrospun membranes, which displayed a controlled release of antibiotics from the nanofibers to provide an aseptic environment at the wound site as well as for promoting the re-epithelialization and new tissue formation (please see Table 1) [33–38].

Alavarse et al. incorporated tetracycline hydrochloride (TCH), at a concentration of 5 mg/mL, into Poly(vinyl alcohol) (PVA)/Chitosan (CS) (80/20 v/v) electrospun nanofibers [36]. A blend of polymer-antibiotic was initially electrospun and then crosslinking using glutaraldehyde vapor (GA) (0.5% for 4 h). This crosslinking step lead to an increase in the fibers mean diameter, from 119 ± 33 nm to 309 ± 68 nm. Further, the authors observed that 80% of TCH was

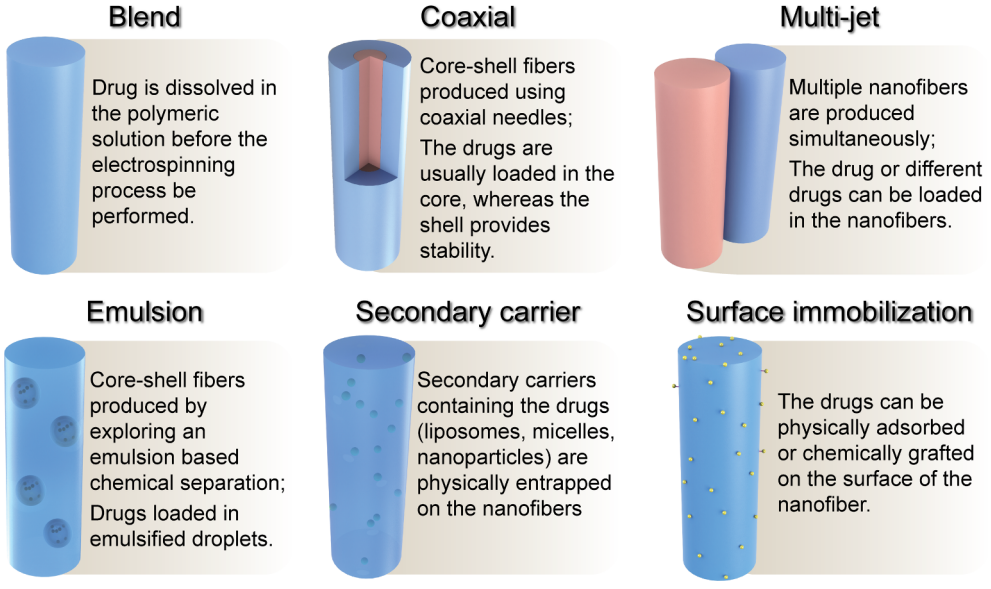

Fig. 1. Illustration of the main strategies used to incorporate drugs into electrospun nanofibers.

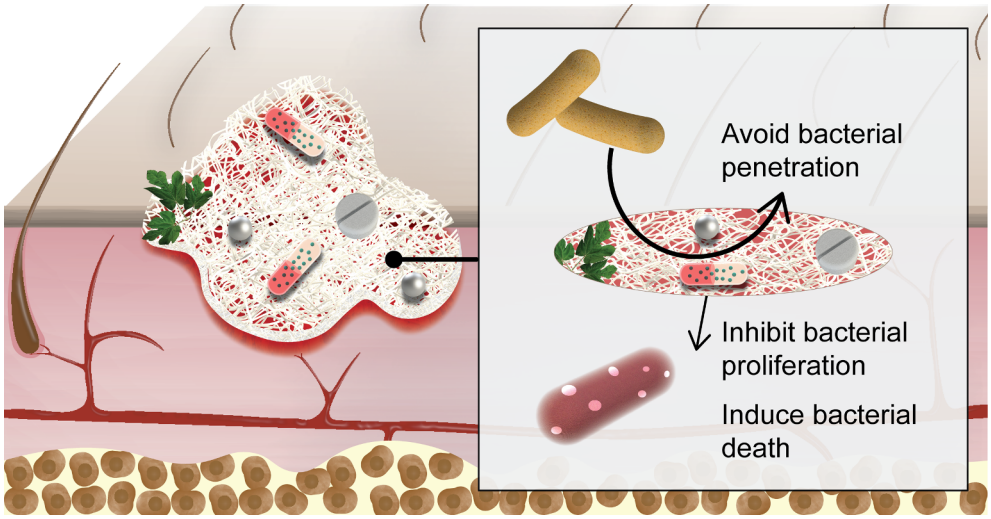

Fig. 2. Illustration of the main antimicrobial agents (antibiotics, silver nanoparticles and natural extracts-derived products) incorporated into the electrospun nanofibers and their role in the healing process.

released from PVA/CS nanofibers in PBS solution (pH 7.4), after 24 h, which corresponds to the critical period for the establishment of wound infections. Moreover, the antimicrobial activity of PVA/CS/TCH membranes was characterized using *Escherichia coli* (*E. coli*), *Staphylococcus epidermis* (*S. epidermidis*) and *Staphylococcus aureus* (*S. aureus*) as model bacteria. The obtained results showed that the incorporation of TCH into the PVA/CS nanofibrous membranes can inhibit the bacterial growth, during 24 h. Additionally, the authors reported inhibitory halos with a diameter of 8.8 ± 0.4 mm for *E. coli*, 15.6 ± 0.3 mm for *S. epidermis* and 19.6 ± 0.2 mm for *S. aureus,* which contrasts with the absence of inhibitory activity displayed by the non-functionalized membranes. In addition, these researchers also noticed that when the drug-loaded nanofibrous membranes were added to rabbit aortic smooth muscle cells, they did not affect the cell viability for at least 72 h.

Torres-Giner et al. produced polylactide (PLA) nanofibers loaded with gentamicin using three different approaches based on the incorporation of gentamicin 5 wt% into PLA nanofibers, PLA-collagen blends or in the collagen core of the collagen-PLA coaxial nanofibers [38]. Their results revealed that PLA fibers containing gentamicin presented a bimodal size distribution with an average diameters of 1106 ± 182 nm and 281 ± 55 nm; gentamicin loaded PLA-collagen blends had fibers with diameters of 168 ± 53 nm; and coaxial PLA-collagen-PLA/gentamicin presented fibers with mean diameter values of 561.43 ± 104 nm and 131.07 ± 39 nm. Moreover, the gentamicin release profile exhibited by all formulations was similar, *i.e.* the antibiotic presented a fast diffusion in the first 24 h, followed by a sustained release until reach the equilibrium after 50 h. Nevertheless, the PLA fibers released 19% of the drug after 24 h, increasing to 33% after the 50 h of incubation. On the other hand, PLA-collagen blends released 78% and 98% of gentamicin after 24 h and 50 h, respectively. Coaxial PLA-collagen-PLA nanofibers released 41% and 59% of gentamicin after 24 h and 50 h, respectively. Further, these researchers also determined the lowest concentration of gentamicin required to prevent the bacterial growth and to kill the bacteria, which are defined as minimal inhibitory concentration (MIC) and minimum bactericidal concentration (MBC), respectively. So, the PLA-collagen blends presented MIC values of 0.25, 5 and 0.5 mg and MBC values of 5, 50 and 25 mg for *S. epidermis*, *Pseudomonas aeruginosa* (*P. aeruginosa*) and *E. coli*, respectively. In turn, the PLA-collagen-PLA coaxial fibers displayed a slightly lower bactericidal activity, exhibiting MIC values of 1, 10, and 0.5 mg and MBC values of 7.5, 50, and 25 mg. PLA fibers presented the lowest antimicrobial activity for the tested bacteria, showing MIC values of 2.5, 25 and 0.5 mg and MBC values of 10, 100, and 50 mg. Moreover, the electrospun PLA-based fibers were also able to provide a matrix that promotes cell proliferation.

Li and their co-workers loaded CIF (0.9%) into thermoresponsive electrospun fiber mats produced with poly(di(ethylene glycol) methyl ether methacrylate) (PDEGMA)/ poly(l-lactic acid-co-ε-caprolactone (P (LLA-CL) [39]. The CIF incorporation into the meshes leads to a variation on the nanofibers size, *i.e.* the non-loaded nanofibers presented diameters ranging from 948 ± 132 nm to 476 ± 189 nm, whilst the fibers containing CIF presented diameters ranging from 330 ± 118 nm to 437 ± 141 nm. Further, the release profile of CIF was characterized by an initial burst (45% of the drug was released in 10 h) that span up to 170 h, reaching a maximum cumulative release of 85%. This behaviour leads to the formation of inhibitory halos, with a diameter of 5.35 ± 0.51 cm and 5.21 ± 0.44 cm for *E. coli* and *S. aureus*, respectively, after 24 h of incubation. These values increased to 5.45 ± 0.81 cm and 5.62 ± 0.53 cm after 72 h of incubation, thus revealing that the antibacterial activity of the fibers remained for at least three days. Moreover, the *in vitro* assays also demonstrated that the nanofibers promote the adhesion and proliferation of L929 fibroblasts. In the *in vivo* assays, the fibers loaded with CIF induced a reduction of the wound area (5.7 ± 0.8% of the original area), a higher expression of CD34 (a marker used to select vascular endothelial cells) and the formation of a thicker epidermis in comparison to commercially available gauzes [39].

Mohseni and their collaborators incorporated SSD into PVA nanofibers for conferring them antimicrobial activity [40]. To accomplish that, different concentrations of SSD (1, 5 and 10 wt%) were added to the PVA solution before the electrospinning process be performed. Afterwards, the nanofibers' diameter was measured and the authors verified that the average diameter of PVA nanofibers increased with the incorporation of SSD, from 360 nm to 450, 530, and 700 nm for the PVA/SSD (1%), PVA/SSD (5%), PVA/SSD (10%) fibers, respectively. Further, the authors observed that 70% of the SSD was released during the first 7 days of incubation, reaching a value close to 100%, after 14 days. Additionally, the membranes displayed a bactericidal activity dependent on the SSD concentration. Inhibitory halos with a diameter of 2 ± 0.2 mm, 3.9 ± 0.5 mm, and 4.2 ± 0.3 mm were obtained for PVA/SSD (1%), PVA/SSD (5%), and PVA/SSD (10%) membranes, respectively (as showed in Fig. 3), when they were added to *S. aureus*. On the other side, these researchers also verified that the incorporation of SSD decreased the mechanical properties of the membranes (the elastic modulus decreased from 56.07 MPa to 36.19 MPa for PVA/SSD (1%),

Table 1
Overview of different antibiotics incorporated into electrospun membranes to be used as wound dressing.

Antibiotic	Polymer	Incorporation method	Fiber diameter (nm)	Release profile	Antibacterial assays	Main conclusions	Refs.
Tetracycline hydrochloride (TCH)	PVA /CS	Blend electrospinning	-PVA/CS: 138 ± 23 nm -PVA/CS/TCH: 119 ± 33 nm	- The release profile of TCH displayed an initial burst release (80%), after 2 h.	-The zone of inhibition obtained was 8.8 ± 0.4 mm, 15.6 ± 0.3 mm and 19.6 ± 0.2 mm for *E. coli*, *S. epidermidis* and *S. aureus*, respectively.	- The TCH-loaded PVA/CS membranes showed good biocompatibility in contact with rabbit aortic smooth muscle cells; - The scratch assay demonstrated a higher cell migration rate (about 8%/h and 6%/h) during the initial 12 h of incubation.	[36]
	Zein/PCL	Blend electrospinning	-Zein 3L: 0.99 ± 0.36 μm - Zein/PCL 3L: 1.51 ± 0.65 μm	- In zein/PCL 3L fibers the TCH was gradually released, reaching the 19% in the first 3 h; -After 20 days, 27% of TCH was released from the nanofibers.	-The 3L matrices significantly reduced the number of living cells (from 100% to ≈ 35%) in the biofilms of MRSA252; -For MRSA (ATCC 25923), the 3L matrices mediated a reduction in the viable cells from 100% to 27%.	- For the first time, TCH loaded matrices were applied in *ex vivo* pig skin models growing MRSA252 or ATCC 25923; -The zein/PCL nanofibers loading with TCH were biocompatible with human fibroblast FEK4 skin cells.	[42]
Gentamicin	PLA/Collagen	Blend electrospinning and coaxial electrospinning	Blend fibers:-PLA-collagen/ gentamicin:168 ± 53 nm Coaxial fibers: - PLA-collagen/ gentamicin: 561 ± 104 nm and 131 ± 39 nm	-In blend PLA-collagen fibers, 78% and 98% of gentamicin was released after 24 h and 50 h, respectively; -In coaxial PLA-collagen-PLA, 41% and 59% of gentamicin was released after 24 h and 50 h, respectively.	- The blend fibers presented MIC values of 0.25, 5 and 0.5 mg and MBC values of 5, 50 and 25 mg for *S. epidermidis*, *P. aeruginosa* and *E. coli* respectively; - The coaxial fibers displayed MIC values of 1, 10 and 0.5 mg and MBC values of 7.5, 50 and 25 mg respectively.	- The *S. epidermidis* presented a superior susceptibility towards gentamicin, followed by E. coli and *P. aeruginosa*; - The electrospun PLA-based fibers promoted a matrix favourable for cell proliferation during 14 days.	[38]
	Chitosan (CS)	-Gentamicin was loaded into liposomes; -Surface chemical immobilization of drug-loaded liposomes at surface of membranes	Not available	-The release of gentamicin from liposomes immobilized at the surface of CS membranes was characterized by a steady release rate after 16 h, which stabilized until 24 h.	- The diameter of inhibition zones exhibited by samples was 21.6 mm, 22.1 mm and 14.1 mm for *S. aureus, E. coli* and *P. aeruginosa*, respectively; - The broth dilution method demonstrated a Log(reduction) = 3.87 ± 0.33 for *S. aureus*, 4.87 ± 0.21 for *E. coli*, and 4.20 ± 0.24 for *P. aeruginosa*.	- The gentamicin released from liposomes immobilized at surface of electrospun CS membranes avoided the growth of *S. aureus, E. coli* and *P. aeruginosa*.	[43]
Ciprofloxacin(CIP)	PLGA/alginate microparticles (ALG)	Blend electrospinning	-ALG(1%) /PLGA: 673 ± 243 nm; -ALG(1%)/PLGA-CIP: 877 ± 431 nm	-A burst release of CIP occurred in the first 7 days, which was followed by a slow release for up to 40–50 days.	-The MIC of ciprofloxacin (1%) was 0.125 μg/mL against *S. aureus*; -The CIP-loaded nanofibers exhibited an inhibition zone ranging from 35 to 45 mm, in contact with *S. aureus*.	- The addition of sodium alginate enhanced the wettability, water uptake potential, facilitating the release of CIP at the early diffusion phase.	[44]
	PDEGMA/P(LLA-CL)	Blend electrospinning	- Fibers without CIF: 948 ± 132 nm to 476 ± 189 nm -Fibers with CIF: 437 ± 141 nm to 330 ± 118 nm	- CIF displayed a burst release (45%) at first 10 h, followed by a gradual release over 170 h; -The final cumulative release of CIF was 81%-85%.	- The diameter of the inhibition zones exhibited by CIF-loaded fibers was 5.35 ± 0.51 cm and 5.21 ± 0.44 cm for *E. coli* and S. *aureus*, respectively; - After 72 h, the diameter of inhibition zones increased for 5.45 ± 0.81 cm and 5.62 ± 0.53 cm for *E. coli* and *S. aureus*, respectively.	- *In vivo* assays revealed that the fibers loaded with CIF had better wound healing performance in comparison with commercial gauze; - The fibers promoted the adhesion and proliferation of L929 fibroblasts.	[39]

(*continued on next page*)

Table 1 (*continued*)

Antibiotic	Polymer	Incorporation method	Fiber diameter (nm)	Release profile	Antibacterial assays	Main conclusions	Refs.
Silver sulfadiazine (SSD)	PCL/PVA	Blend electrospinning	-PVA: 360 nm −1–10 wt% SSD/ PVA:450–700 nm	- The release profile of silver showed a burst release in the initial 24 h; -70% of silver was released during the first week, followed by a gradual release during the second week.	- The largest inhibition halo against *S. aureus* (4.2 ± 0.3 mm) was observed in 10 wt% SSD/ PVA membranes, while the smallest inhibition zone (2.0 ± 0.2 mm) was presented by 1 wt% SSD/PVA fibers.	- The cellular proliferation was strongly influenced by SSD concentration, where the highest amount of SSD promoted the lowest cell proliferation; - All the membranes showed good mechanical properties (young modulus: 56.07 to 18.14 MPa) and wettability (contact angle inferior to 90).	[40]

27.52 MPa for PVA/SSD (5%), and 18.14 MPa for PVA/SSD (10%)) and increased the hydrophilic character of their surfaces.

However, in recent years researchers and clinicians have been facing the emerging of multidrug resistant bacteria that arise as a consequence of the continued administration of antibiotics. In fact, more than 70% of the bacteria responsible for wound infections are resistant to at least one of the antibiotics used nowadays in the clinic [41]. Such drawback demands the development of new antimicrobial alternatives that can be used for the treatment of skin infections.

3.2. Silver nanoparticles

The recent advances of nanotechnology-based therapies have paved the way for fighting microorganisms' multidrug resistance. In particular AgNPs have been emerging as a promising alternative to the use of antibiotics. In fact, the excellent antimicrobial properties displayed by AgNPs have been already tested against 650 different strains of bacteria [17,45,46]. So far, four mechanisms have been proposed to explain the antimicrobial activity of this type of nanoparticles: (i) AgNPs are able to adhere onto the surface of bacterial cell wall, causing changes in cell membrane structure and permeability, that lead to the leakage of the cellular content; (ii) AgNPs can enter into cell cytoplasm and induce damages in the intracellular structures (such as mitochondria, vacuoles, ribosomes) and biomolecules (*e.g.* protein, lipids, and DNA); (iii) AgNPs can mediate the production of reactive oxygen species (ROS) and free radicals; and (iv) AgNPs can modulate the signal transduction pathways, inducing the phosphorylation of various proteins in bacteria and ultimately trigger the cell death [47–49]. The antibacterial activity unveiled by AgNPs encouraged the researchers to produce different silver-based wound dressings that are already available in the market, like Acticoat®, Aquacel Ag®, Silvasorb®, and Silvercel™ [17]. Furthermore, AgNPs have been also incorporated into electrospun membranes to confer them antimicrobial properties (see Table 2 for further details). Aadil and colleagues produced PVA-lignin nanofibers containing AgNPs (with diameters ranging from 10 to 50 nm) using the electrospinning technique [50–52]. The diameter of the produced nanofibers varied between 128 and 291 nm and the presence of the AgNPs within these nanofibers was confirmed through the observation of the two characteristic diffraction peaks at 33 and 47° in the X-ray spectrum, corresponding to the {1 1 1} and {2 0 0} planes of silver, respectively. Moreover, the antimicrobial activity of the produced membranes was checked against *E. coli* and *Bacillus circulans* (*B. circulans*). Santos et al. immobilized AgNPs on the surface of Polycaprolactone (PCL)/poly[(2-dimethylamino)ethyl methacrylate] (PDMAEMA) nanofibrous membranes, following the methodology proposed by Dong et al. [53,54]. Further, the AgNPs size and nanoparticles content on the PCL/PDMAEMA were optimized by varying the pH values (1, 3, 5, 7, and 9) of the growth solution. In fact, the diameter of AgNPs decreased from 1020 ± 60 nm at pH 1 to 64 ± 3 nm at pH 9. On the other side, the pH also influenced the amount of AgNPs adsorbed at the surface of the nanofibers, i.e, 0.59 ppm, 7.40 ppm, 10.1 ppm, 3.40 ppm, and 0.12 ppm of silver was adsorbed at the nanoparticles surface at pH 1, 3, 5, 7 and 9, respectively. Thus, AgNPs showed the maximum adsorption at pH 5, which was attributed to the increased electrostatic interactions that occur between the positively charged amino groups of PDMAEMA and the negatively charged carboxylate groups of citrate present on the surface of AgNPs. Moreover, the results obtained revealed that the biocompatibility of the meshes increased after the AgNPs immobilization and they were able to inhibit the growth of *S. aureus*, *P. aeruginosa*, and *E. coli* [54].

Lee et al. produced CS nanofibers containing different amounts of AgNPs (0, 0.7, 1.3, 2 and 4%) [55]. To accomplish that, AgNPs were produced directly in the CS solution, through the chemical reduction of silver nitrate using sodium borohydride. The obtained spherical AgNPs presented an average diameter of 10 ± 2 nm and presented a narrowed wavelength band at 408 nm in UV–vis absorption spectra, which is

a)

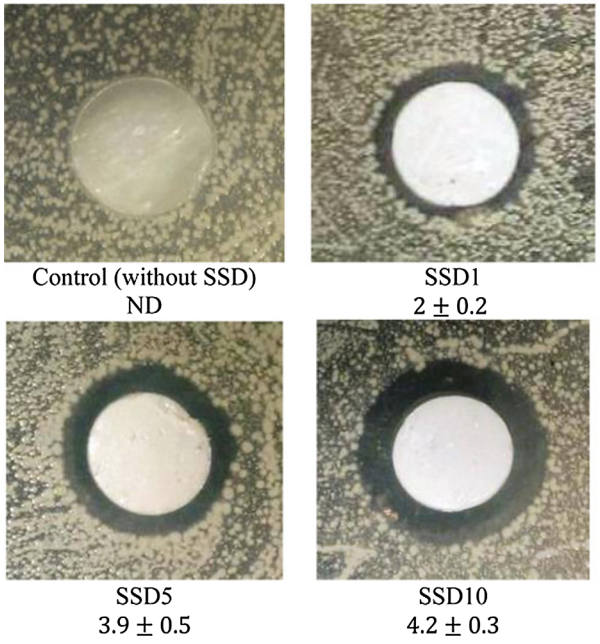

b)

Commercialized wound dressing	Inhibition Zone
Biohesive Ag	0.2 ± 0.1
Aquacel® Ag	0.6 ± 0.2
Algisite Ag	1 ± 0.2
Mepilex® Ag	ND
PolyMem® Ag	ND

Fig. 3. Characterization of the antibacterial activity SSD loaded PVA electrospun mats against *S. aureus*. The inhibitory halos produced by the electrospun nanofibers containing different concentrations of SSD are presented in (a) and the bactericidal activity of commercially available wound dressings are shown in (b). Reproduced from [40] with permission from Wiley.

characteristic of small-diameter AgNPs. Further, the AgNPs formation was also confirmed by X-ray diffraction being observed the presence of peaks at 38.0°, 44.3°, 64.5° and 77.2°, characteristic of the {1 1 1}, {2 0 0}, {2 2 0} and {3 1 1} planes of the AgNPs with a face centered cubic structure. The obtained data showed that a higher content of AgNPs induces a decrease in the nanofibers' diameter from 460 ± 80 nm (at 0%) to 126 ± 28 nm (at 4%). However, nanofibers containing 4% of AgNPs displayed beads and a tangled surface morphology, thus causing their removal from the antibacterial assays. *P. aeruginosa* and Methicillin-resistant *Staphylococcus aureus* (MRSA) were used as model bacteria to characterize the antimicrobial activity of the produced nanofibers, as can be observed in Fig. 4. The diameter of the inhibitory halo increased from 0 mm to 16.07 mm, 16.58 mm, and 16.73 mm in *P. aeruginosa* and from 0 mm to 14.9 mm, 15.42 mm and 15.75 mm in MRSA when increasing amounts of AgNPs were incorporated in the nanofibers (0, 0.7, 1.3 and 2%, respectively).

Despite the promising bactericidal activity displayed by silver loaded nanofibrous membranes, there are some handicaps that avoid their widespread in the clinic [56]. Indeed, the AgNPs have some degree of cytotoxicity and the long-term interactions with the human body, besides the nanoparticles fate, is poorly understood.

In this field, several studies have been focused on understanding the possible toxic effects of metallic nanoparticles for skin tissue. The metallic nanoparticles-skin interaction (*i.e.* penetration and toxicity) are largely influenced by different physicochemical properties such as the particle type, size, shape, surface coating, charge, stability, and protein corona among others [57–59]. Once the metal nanoparticles become infiltrated into the skin, they can trigger several toxic effects by inducing cell oxidative stress, apoptosis and mitochondrial dysfunction, as well as membrane and DNA damage. In addition, the metallic ions released from the nanoparticles may cause skin sensitization and irritation [60–62]. However, until now the data available concerning the toxicity of metallic nanoparticles is insufficient, demanding in-depth studies to evaluate their biosafety.

3.3. Natural extracts-derived products

To overcome the limitations associated with the use of antibiotics and silver nanoparticles, researchers have been testing a wide variety of natural products that have been loaded into electrospun membranes (Table 3). Amidst them, plant extracts and essential oils (EOs) have been screened as potential sources of novel antimicrobial compounds [67–71]. The antimicrobial properties exhibited by EOs is mainly attributed to the presence of active constituents such as terpenes, terpenoids, and other aromatic and aliphatic constituents [72,73]. Moreover, the hydrophobic character of the EOs and their components promote the partition of the lipids present in the cell membrane, increasing their permeability and consequently leading to the bacterial cells death due to the leakage of essential molecules and ions [71,74,75]. Therefore, the EOs can act as powerful tools to circumvent the bacterial multi-drug resistance [76]. Liakos et al. reported the incorporation of three different EOs (cinnamon (CN), lemongrass (LG) and peppermint (PM)) into Cellulose Acetate (CA) electrospun nanofibers [77]. The produced fibers were free from defects or beaded structures, presenting a mean diameter of 4.2 ± 2.1 μm, 0.9 ± 0.3 μm, 2.8 ± 1.1 μm, and 2.3 ± 0.8 μm for pure CA, CA/5-CN, CA/5-LG, and CA/5-PM, respectively. Furthermore, while the pure CA fibers were colonized by *E. coli* and *Candida albicans* (*C. albicans*), leading to the formation of biofilms. Fibers loaded with 6.2 and 25% w/w of EOs were able to impair *E. coli* growth since a clear inhibition zone was observed around the samples. On the other hand, the inhibition of *C. albicans* growth was only accomplished when the EOs concentration was increased to about 40% w/w.

Recently, Miguel and collaborators incorporated thymol (THY) into an electrospun Silk Fibroin (SF) based asymmetric membrane to confer it antioxidant and antibacterial properties [8]. For that purpose, THY (5 mg/mL) was directly mixed with SF and hyaluronic acid (HA) blend before the electrospinning process. The incorporation of THY within these nanofibers induced an increase in the fibers mean diameter from 306.8 ± 85.6 nm to 412.7 ± 106.7 nm. Additionally, the encapsulation efficiency of THY was 79.7 ± 7.19%. Further, the authors observed that the THY release profile is pH dependent, with 71.25 ± 2.06% and 91.87 ± 0.99% of THY molecules being released after 24 h of incubation at pH 5 and pH 8, respectively. Moreover, the antioxidant properties of the nanofibers were evaluated, revealing that the THY incorporation into the nanofibers conferred ≈ 45.64% of antioxidant activity, as well as inhibited the *S. aureus* and *P. aeruginosa* growth in 87.42% and 58.43%, respectively (as represented in Fig. 5). In addition, the SF_HA_THY membranes induced larger inhibitory halos in *S. aureus* and *P. aeruginosa* than those obtained with SF_HA

Table 2
Description of different electrospun meshes incorporating silver nanoparticles aimed to be used as wound dressing.

Bioactive molecule	Polymer	Incorporation method	Fiber diameter (nm)	Antibacterial assays	Main conclusions	Refs.
Silver nanoparticles (AgNPs)	PVA/lignin	Blend electrospinning	- PVA/lignin/AgNPs: 128–291 nm	- The zone of inhibition was 1.1 ± 0.05 cm against *E. coli* and 1.3 ± 0.08 cm against *B. circulans*.	- The nanofibers presented yellow and uniform appearance, due to the presence of lignin and AgNPs; - The TEM analysis revealed that AgNPs presented a diameter ranging from 10 to 50 nm.	[50]
	PCL/ PDMAEMA	Blend electrospinning and *in situ* formation and immobilization of AgNPs	- PCL/PDMAEMA (80:20): 410 ± 160 nm - PCL/PDMAEMA (50:50): 330 ± 170 nm	- The membranes containing AgNPs showed inhibition halos against *S. aureus*, *P. aeruginosa*, and *E. coli*.	- The AgNPs immobilization was more efficient at pH 5 (≈ 25% of adsorption efficiency); - The AgNP immobilization improved the biocompatibility of the membranes.	[54]
	Chitosan (CS)	Blend electrospinning	- CS = 460 ± 80 nm - CTS/AgNPs (4%) = 349 ± 56 nm - CTS/AgNPs (1.3%): 337 ± 49 nm - CS/AgNPs (2%): 238 ± 46 nm - CS/AgNPs (4%): 126 ± 28 nm	- CTS/AgNPs nanofibers containing 0.1, 1.3 and 2% of AgNPs presented inhibition halos of: 16.07 mm, 16.58 mm and 16.73 mm, against *P. aeruginosa*; 14.9 mm, 15.42 mm and 15.75 mm against MRSA, respectively.	- The TEM analysis revealed that the spherical AgNPs with diameter of 10 ± 2 nm were well dispersed in the fibers; - The increase in the AgNPs concentration improved the nanofibers antibacterial effect.	[55]
	Collagen	Blend electrospinning	Not available	- After 48 h, the inhibition zones were: 3.2 ± 0.3 cm in *S. aureus* and 2.3 ± 0.3 cm in *P. aeruginosa*; - The MIC values of AgNPs against *S. aureus* and *P. aeruginosa* were 5.8 ± 0.3 μg/ml and 7.4 ± 0.2 μg/ml respectively.	- The entrapment efficiency of AgNPs into nanofibers was 88.1 ± 0.7%; - The AgNP loaded nanofibers showed excellent wound-healing efficacy due to their intrinsic antibacterial, anti-inflammatory, controlled drug release profile and hemostatic properties.	[63]
	CS/PVA	Blend electrospinning	- CS/PVA: 155 nm - CS/PVA/ 0.25% AgNPs: 148 nm - CS/PVA/ 0.5% AgNPs: 144 nm - CS/PVA/ 1% AgNPs: 139 nm	- The inhibition zones against *E. coli* were 7.7, 13.3 and 9.0 mm in CS/PVA/AgNPs (0.25, 0.5 and 1%) respectively; - The inhibition zones against *S. aureus* were 9.1, 14.3 and 8.5 mm in CS/PVA/AgNPs (0.25, 0.5 and 1%) respectively.	- The CS/PVA/AgNPs (0.5%) nanofibers showed the highest tensile strength; - The cumulative release of Ag from the electrospun nanofibers was 40, 56 and 36% after 16 days for nanofibers loaded with 0.25, 0.5 and 1% of AgNPs, respectively.	[64]
	PVA/Collagen (COS)	Blend electrospinning	- PVA/COS (2:1): 192.57 ± 59.30 nm - PVA/ COS-AgNPs: 130.13 ± 43.55 nm	- The PVA/COS-AgNP nanofibers showed clear inhibition zones against *S. aureus* and *E. coli*.	- The Ag was rapidly released during the first 8 h (≈ 80%), which continued gradually thereafter (≈ 100% after 120 h); - The cytotoxicity tests showed that PVA/COS-AgNPs presented excellent *in vitro* biocompatibility in contact with fibroblasts cells; - The PVA/COS-AgNPs nanofibers accelerated the early stages of wound healing.	[65]
	CS/PEO	Blend electrospinning	- CS/PEO: 302 ± 56 nm - CS/PEO/Ag (2%): 277 ± 46 nm - CS/PEO/Ag (4%): 258 ± 31 nm - CS/PEO/Ag (8%): 333 ± 56 nm	-The inhibition zones against *E. coli* (≈ 25 mm) were higher than those against *S. aureus* (≈ 15 mm).	- The release profile of Ag from the nanofibers exhibited an initial fast release in first 12 h, followed by a sustained release until the 72 h; - *In vitro* cytotoxicity assays indicated that CS/PEO/Ag nanofibers presented excellent cytocompatibility in contact with pig iliac endothelial cells.	[66]

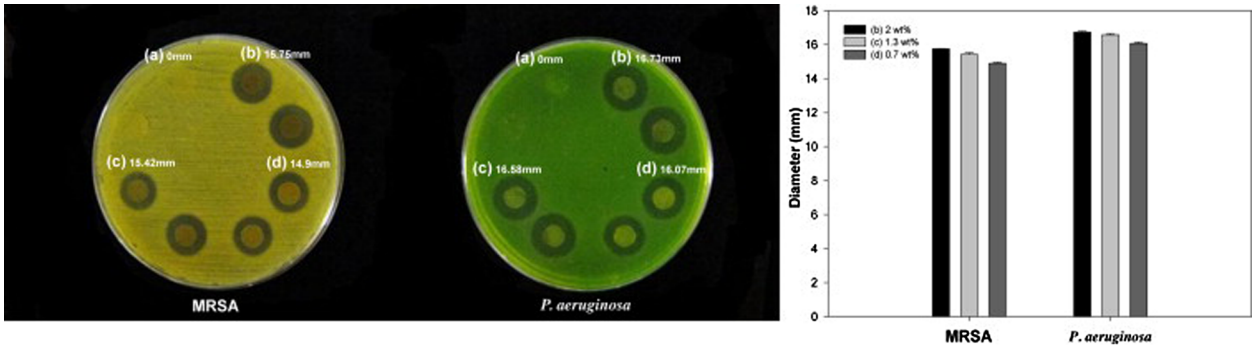

Fig. 4. Analysis of the antibacterial activity of CS/AgNPs membranes against MRSA (dark yellow) and *P. aeruginosa* (green): visualization and measurement of the inhibitory halos of the membranes containing AgNPs at a concentration of 0% (a), 2% (b), 0.7% (c) and 1.3% (d). Reproduced from [55] with permission from Elsevier. (For interpretation of the references to colour in this figure legend, the reader is referred to the web version of this article.)

membranes.

Besides the utilization of EOs, propolis extracts (a resinous mixture produced by honey bees) also displays antibacterial, antifungal, antiviral, antioxidant, and anti-inflammatory properties due to the presence of a wide variety of chemical compounds, such as flavonoid aglycones, phenolic acids, and ester derivatives [78]. Kim et al. prepared a blend of propolis extract (5, 10 and 30% wt) and polyurethane (PU) 10% wt to create a nanofibrous membrane aimed to be used as a wound dressing [79]. The incorporation of the propolis was responsible for an increase in the fibers average diameter 204.4, 321.4, 377.2 and 556.6 nm for PU fibers containing 0, 5, 10, and 30% of propolis, respectively. A higher content of propolis extracts within the PU nanofibers induced a superior bactericidal activity against *E. coli*, with the highest inhibitory effect being registered for the PU membrane containing 30 wt% of propolis [79].

Aloe vera (AV) and CS comprise other examples of sources from natural compounds displaying antimicrobial activity [3,7,80,81]. The amino acids, salicylic acid, ascorbic acid, vitamin A (Vit-A), and vitamin E (Vit-E) found in AV confers it antibacterial, anti-inflammatory, and antioxidant activity [82,83]. On the other hand, CS is a natural-derived polysaccharide that promotes collagen synthesis and exhibits bactericidal and hemostatic properties [3,84]. Despite different mechanisms have been proposed for explaining the antimicrobial activity presented by CS, the most accepted mechanism is based on the establishment of electrostatic interactions between positively charged amine groups of CS and the negatively charged groups present in the bacterial cell wall, leading to an increased cell wall permeability, leakage of intracellular constituents and the dissipation of the ionic gradients of bacteria [3,85,86]. Miguel et al. produce electrospun nanofibers using a blend of extract AV (40% v/v) and CS_ poly(ethylene oxide) (PEO) [7]. The incorporation of the AV extract resulted in the production of thinner fibers, *i.e.* the mean diameter of the fibers decreased from 239 ± 122 nm to 152 ± 54 nm. Moreover, both CS_PEO and CS_AV_PEO membranes were able to inhibit *S. aureus* and *E. coli* growth as well as avoid biofilm formation at the membranes' surface. In 2016, Sarhan and collaborators studied the antibacterial and wound healing activity of honey, by performing its incorporation into PVA/CS nanofibers [87]. The results obtained demonstrated that higher contents of honey (10, 20 and 30%) induced the formation of fibers with increased diameters (284 ± 97 nm, 371 ± 110 nm, and 464 ± 185 nm, respectively). Moreover, the nanofibers containing 30% of honey were the ones unveiling a higher antibacterial activity against *S. aureus* and *E. coli*.

4. Bioactive molecules that have been incorporated into electrospun membranes aiming to improve the healing process

The skin regeneration process is comprised of five main phases: haemostasis, inflammation, migration, proliferation, and remodelling. These phases involve a complex interaction between cells (*e.g.* neutrophils, macrophages and fibroblasts), GFs and cytokines [98]. To improve this process, researchers have been incorporating bioactive molecules into electrospun membranes [1,99–101]. The controlled and targeted release of biological molecules (*e.g.* GFs, vitamins, and anti-inflammatory molecules) at the wound site is fundamental for the regulation of the wound healing process (as illustrated in Fig. 6) [102].

4.1. Growth factors

GFs are biologically active polypeptides that are able to regulate the cell growth, differentiation, proliferation, migration and metabolism during the wound healing process [103]. All phases of the wound healing process are controlled by a wide variety of GFs and cytokines, particularly, epidermal growth factor (EGF), platelet derived growth factor (PDGF), transforming growth factor-β (TGF- β), fibroblast growth factor (FGF), and vascular endothelial growth factor (VEGF) [104–107]. These molecules play a critical role in the formation of the granulation tissue, in the modulation of the inflammatory response (*e.g.* PDGF, TGF- β, and interleukins (*e.g.* IL-1 and IL-6)) as well as in the promotion of angiogenesis (*e.g.* EGF and VEGF). Moreover, GFs are also required for the ECM formation and remodelling as well as for the re-epithelialization processes (*e.g.* FGF, EGF, and VEGF) [106]. Nevertheless, the topical administration of GFs presents several drawbacks such as low *in vivo* stability, restricted absorption through the skin, elimination by exudation before reaching the wounded area, and undesirable side effects due to high local and/or systemic levels. Therefore, the loading of GFs into nanofibers is regarded as an appealing strategy for improving the wound healing process [30,108]. In Table 4 are presented different electrospun membranes functionalized with GFs aimed to be used as wound dressings.

Norouzi et al. explored the application of the multi-jet electrospinning technique to create core-shell nanofibrous membranes containing poly(lactic-co-glycolic acid (PLGA)-EGF and gelatin for improving skin regeneration [109]. The produced membranes presented PLGA-EGF and gelatin nanofibers with diameters of 390 ± 75 nm and 175 ± 45 nm, respectively. Further, the combination of PLGA and gelatin nanofibers improved the swelling ability of the membranes, from 23 ± 4% for pure PLGA fibers to 130 ± 10% for PLGA/gelatin nanofibrous membranes. Additionally, the release of EGF from these membranes occurred through an initial burst release, followed by the sustained release over 9 days. Moreover, these membranes were also able to improve the blood clotting, cell adhesion, and proliferation as well as enhance the collagen type I and III expressions (the expression levels of this protein were 22 and 25 times higher than in the normal cells).

Piran and their coworkers encapsulated PDGF into CS nanoparticles (CS-NPs) and then blended them on a PCL solution, that was subsequently electrospun [110]. The data obtained showed that the addition

Table 3
List of several types of electrospun membranes incorporating natural extracts-derived products to provide antibacterial properties to wound dressing.

Bioactive molecule	Polymer	Incorporation method	Fiber diameters	Antibacterial assays	Main findings	Refs.
Thymol (THY)	SF_HA	Blend electrospinning	- SF_HA nanofibres: 306.8 ± 85.6 nm - SF_HA_THY nanofibres: 412.7 ± 106.7 nm	- The SF_HA_THY membranes exhibited an increased antibacterial efficiency, 87.42% and 58.43% for *S. aureus* and *P. aeruginosa*, respectively; - The SH_HA_THY layer displayed a 2 to 3 times larger inhibitory halo area in comparison to SF_HA for *S. aureus* and *P. aeruginosa*, respectively.	- The release profile of THY from SF_HA nanofibers was 71.25 ± 2.96% and 91.87 ± 0.99% at pH 5 and pH 8, respectively; - The SF_HA_THY membrane presented a high antioxidant activity (≈ 45.64%); - *In vitro* assays demonstrated that the membrane promoted the cell adhesion and proliferation.	[8]
	PCL/PVA	Co-axial electrospinning	- PCL/PVA nanofibers: 238 ± 23 nm - PCL/PVA/THY (5%) nanofibers: 477 ± 51 nm - PCL/PVA/THY (10%) nanofibers: 798 ± 88 nm	- The presence of THY in the fibers core resulted in the growth inhibition of *S,aureus* and *E. coli* (greater than99%).	- The THY incorporation induced a decrease in the tensile strength and increased the porosity and pore size; - The fibroblast cells remained viable (greater than90%) in contact with nanofibers during 7 days.	[88]
Cinnamon, clove and lavender	PVA/SA	Blend electrospinning	Not available	- A higher concentration of the oils resulted increased inhibition zones against *S. aureus*; - The fibers containing 1.5% of cinnamon oil, clove oil or lavender oil exhibited a inhibition zone against *S. aureus* of 27.6 mm, 26.6 mm and 20.6 mm, respectively, .	- FTIR spectra exhibited the peaks of oils and polymers, indicating the successful incorporation of oils into the fibers; - Nanofibers containing cinnamon oil showed better antimicrobial properties against *S. aureus* in comparison to clove and lavender oil.	[89]
Rosemary(R) and oregan (Or)	CA	Blend electrospining	- CA nanofibers: ≈ 800 nm - CA_5%R nanofibers: ≈ 1200 nm - CA_5% Or nanofibers: ≈ 1300 nm	- In *S. aureus*, both essential oils (at 5% of concentration) presented similar results, with $1x10^9$ CFU/mL of viable microbial cells after 24 h of incubation; - In *E. coli*, the fibers containing Or presented a lower number of viable bacterial cells (≈ 1×10^6 CFU/ml), exhibiting an improved antibacterial effect; - In *C. albicans*, the fibers containing Or exhibited a pronounced antibacterial effect (about 100 CFU/ml of viable cells).	- The Ramman spectrum revealed that R and Or essential oils were efficiently incorporated into electrospun fibers; - The Or was more effective against S. aureus, E. coli and C. albicans in comparison with the R.	[90]
Cinnamon	PVP	Emulsion electrospinning	- PVP nanofibres: 323.0 ± 69.9 nm - PVP/4% of cinnamon: 401.4 ± 108.7 nm	- The largest inhibition halos were observed for the PVP/4% of cinnamon membranes on *S. aureus*; - For *E. coli*, the PVP/2% of cinnamon presented the higher inhibition zone; - For *C. albicans*, the zone diameters were similar for PVP containing 2%, 3% and 4% of cinnamon.	-The PVP nanofibers containing 2, 3 and 4% of cinnamon exhibited excellent antibacterial effects against *S. aureus*, *E. coli* and *C. albicans*; - No zone inhibition was visualized for *P. aeruginosa*; - The antibacterial activity increased with the size of the electrospun membrane.	[91]
Cinnamon (CN), lemongrass (LG) and peppermint (PM)	CA	Blend electrospinning	- CA nanofibers: 4.2 ± 2.1 μm - CA/5-CN nanofibers: 0.9 ± 0.3 μm - CA/5-LG nanofibers: 2.8 ± 1.1 μm - CA/5-PM nanofibers:2.3 ± 0.8 μm	- The fibers incorporating 6.2 and 25% of EOs were able to inhibit the proliferation of *E. coli*; - The fibers containing 40% of EOs hindered the growth of *C. albicans*.	- The effective encapsulation of the EOs into the fibers was demonstrated by Raman spectroscopy;-The fibers encapsulating low amounts of EOs were able to inhibit the formation of *E. coli* biofilms; - The nanofibers did not induce any cytotoxic effect in contact with fibroblasts and human keratinocytes.	[77]
Lavender	PAN	Blend electrospinning	- PAN nanofibers: ≈ 143.4 nm - PAN/lavender (0.1%) nanofibers: ≈ 141.4 nm - PAN/lavender (0.3%): ≈ 88.55 nm	- PAN/lavender nanofibers presented a clear zone of inhibition with 14–15 mm of the diameter, against *S. aureus* and *K. pneunoniae*; - The MIC determined for lavender oil was 100 $\mu g.mL^{-1}$; - The zone inhibition (13–14 mm) remained unaltered for more than 30 days.	- The cell viability of mouse fibroblasts remained near 100% till 200 $\mu g.mL^{-1}$ of lavender; - The drug release kinetics was fitted to the Higuchi model, and 38% of the lavender oil was released from nanofibers, within 24 h of incubation.	[92]
Tea tree and manuka	PLA	Blend electrospinning	Not available	- The PLA nanofibers without EO and incorporating tea tree oil were not able to inhibit the *S. epidermis* proliferation; - The PLA nanofibers containing manuka oil presented an inhibition zone of 2 cm in diameter.	- The Raman spectroscopy analysis showed that the main components of manuka oil were stable after electrospinning process; - In tea tree oil was observed a strong reduction in the intensity of the Raman spectroscopy characteristic peaks;	[93]

(*continued on next page*)

Table 3 (*continued*)

Bioactive molecule	Polymer	Incorporation method	Fiber diameters	Antibacterial assays	Main findings	Refs.
AV and CS	PEO	Blend electrospinning	- CS_PEO nanofibers: 239 ± 122 nm - CS_AV_PEO nanofibers: 152 ± 54 nm	- Both CS_PEO and CS_AV_PEO exhibited higher antibacterial activity for *S. aureus* (99.59% and 99.99%) and *E. coli* (99.54% and 99.97%), respectively; - No biofilm formation was noticed at surface of membranes.	- The incorporation of AV into the bottom layer of asymmetric membranes provided an adequate moisture at wound site and promoted a better and faster fibroblast attachment and proliferation; - The intrinsic antibacterial properties of CS and AV allowed to produce a bottom layer capable of avoiding the microorganism invasion, while conferring bioactive properties.	[7]
Propolis	PU	Blend electrospinning	- PU nanofibers: 204.4 nm - PU/propolis (5%) nanofibers: 321.4 nm - PU/propolis (10%) nanofibers: 377.2 nm - PU/propolis (30%) nanofibers: 556.6 nm	- The PU membrane containing 30% of propolis exhibited the largest inhibition zone in contact with *E. coli*.	- The tensile strength of the nanofibers decreased when the concentration of propolis increased; - The propolis incorporation within nanofibers increased the hydrophilicity of the composite PU membranes; - The membranes allowed the proliferation and adhesion of fibroblast cells.	[79]
Aloe vera (AV)	Gelatin (Gel); PCL	Blend electrospinning; Co-electrospinning	- Gel/AV nanofibers: 124.8 ± 43.1 nm	- The Gel/AV-PCL presented an inhibition zone of 20 mm and 15 mm for *S. aureus* and *E. coli*, respectively; - The Gel/AV-PCL nanofibers presented greater than 99% and 85.63% antibacterial activity against *S. aureus* and *E. coli*, respectively.	- The membranes containing 10% of AV showed the highest biodegradation rate (up to 29% after 4 weeks immersion); - The AV incorporation improved the fibroblast proliferation in comparison to PCL and Gel-PCL membranes.	[94]
Manuka honey (MH)	SF	Blend electrospinning	- SF nanofibers: 484.28 ± 101.04 nm - SF/MH (10%) nanofibers: 843.92 ± 146.30 nm - SF/MH (30%) nanofibers: 1149.43 ± 205.03 nm - SF/MH (50%) nanofibers: 1547.72 ± 338.60 nm - SF/MH (70%) nanofibers: 2229.33 ± 399.20 nm	- The MH (10%), MH (30%), MH (50%) and MH (70%)/SF nanofibrous membranes presented inhibition zones against *E. coli* (2.5 mm, 4.2 mm, 5.7 mm and 7.6 mm); *S. aureus* (1.1 mm, 1.7 mm, 2.7 mm and 4.5 mm); *P. aeruginosa* (1.3 mm, 3.7 mm, 6.3 mm and 8.3 mm); *MRSA* (0.7 mm, 1.6 mm, 5.5 mm and 6.7 mm), respectively; - The bacterial inhibition efficacy against *E. coli* was (1%, 10%, 24%, 37% and 51%), *S. aureus* (1%, 6%, 12%, 23% and 29%), *P. aeruginosa* (1%, 8%, 19%, 42% and 57%) and *MRSA* (2%, 7%, 13%, 32% and 40%) for MH (10%), MH (30%), MH (50%) and MH (70%)/SF nanofibrous membranes, respectively.	- The increase in MH amount incorporated into SF fibrous matrices did not affect the cell viability; - The MH incorporation enhanced the adhesion and spreading of fibroblasts at membranes' surface; - *In vivo* assays, the MH/SF nanofibrous membranes improved the healing process, showing a similar effect to that of the AquacelAg dressing.	[95]
Honey/CS	PVA	Blend electrospinning	Not available	- The antibacterial activity was dependent on the CS concentration; - The complete bacterial inhibition was achieved (8.25 for *S. aureus* and 2.9 for *E. coli*) after 48 h of incubation, with the 5.5% of CS.	- The nanofibers displayed antibacterial activity against *S. aureus* but poor antibacterial activity against *E. coli*; - The nanofibers containing 3.5% of CS and 20% honey presented the highest swelling (197%); - The degradation rate of membranes was inversely related to the CS concentration present within nanofibers.	[96]
Honey	PVA/CS	Blend electrospinning	- PVA/CS/honey (10%) nanofibers: 284 ± 97 nm - PVA/CS/honey (20%) nanofibers: 371 ± 110 nm - PVA/CS/ honey (30%) nanofibers: 464 ± 185 nm	- At bacterial concentration of 1×10^8 CFU/ml, the honey just improved the antibacterial activity against *S. aureus*. In *E. coli* assays, no significant improvements were observed.	- The nanofibers containing honey (30%) presented the higher swelling capacity; - The nanofibers degradation increased with higher concentrations of honey.	[87]
CS	PCL/P (MMA-MA)	Coating	- PCL nanofibers: 500 nm - PCL/P(MMA-MA) nanofibres: 350 nm	- The chitosan-coated fibers promoted the death of *E. coli*, within 1 h after the beginning of the experiment; - No growth of bacterial colonies were observed in chitosan-covered fibers after incubation in a bacterial solution.	- The coating of CS circumvented the difficulty of directly electrospinning CS; - The blend between PCL and P(MMA-MA) allowed the deposition of more CS.	[80]

(*continued on next page*)

Table 3 (*continued*)

Bioactive molecule	Polymer	Incorporation method	Fiber diameters	Antibacterial assays	Main findings	Refs.
Garcinia mangostana (GM)	CS-EDTA/PVA	Blend electrospinning	- CS-EDTA/PVA nanofibers: 205.5 ± 36.06 nm - CS-EDTA/PVA/GM (1%-3%) nanofibres: 207.8 ± 34.30 nm-251.3 ± 47.95 nm	- The 1% GM, 2% GM and 3% GM membranes MIC and MBC values were 2 mg/mL, 1 mg/mL and 0.5 mg/mL for *S. aureus* and *E. coli*, respectively.	- The lower swelling ability (96.67%) was noticed in nanofibers containing 3% of GM; - The cumulative release of GM from nanofibers reached 80% after 60 min of incubation; - The membranes are non-toxic and accelerated the healing process.	[97]

of CS-NPs to the PCL solution lead to an increase on the fibers mean diameter (0.76 ± 0.37 μm, 1.22 ± 0.78 μm, and 1.21 ± 0.66 μm for PCL, PCL/CS-NPs and PCL/CS-NPs(PDGF) membranes, respectively). Furthermore, the PDGF release occurred in a controlled and sustained manner, with 12% of PDGF being released after 24 h and reaching a maximum of 83% after 1 week. Besides, it was also reported that the presence of PDGF into PCL/CS-NPs(PDGF) membranes can trigger an higher expression of PDGFRβ gene, more than 2-fold, which will improve the fibroblast cells migration to the injured site. Jin et al. incorporated multiple epidermal induction factors (EIF) like EGF, insulin, hydrocortisone and retinoic acid on gelatin/ poly(l-lactic acid)-co-poly-(ε-caprolactone) (PLLCL) nanofibers using two different approaches: EIF were directly mixed with gelatin/PLLCL composition, resulting in blend nanofibers (gelatin/PLLCL/EIF (b)); or loaded into core-shell fibers of gelatin and PLLCL (gelatin/PLLCL/EIF (cs)) [111]. The authors obtained uniform nanofibers of PLLCL, gelatin/PLLCL, gelatin/PLLCL/EIF (b) gelatin/PLLCL/EIF (cs) with fiber diameters of 456 ± 62 nm, 382 ± 100 nm, 299 ± 46 nm and 366 ± 125 nm, respectively. Further, the authors also observed that in the gelatin/PLLCL/EIF (b) nanofibers, produced through blend electrospinning, occurs an initial burst release of EGF (first three days) that stabilized until day 6, reaching the maximum of 77.8% after 15 days of incubation, which is appropriate for promoting cell proliferation. On the other side, the cumulative release profile of EGF from core-shell gelatin/PLLCL/EIF (cs) nanofibers, did not display the initial burst release, and a stable and sustained diffusion of EGF was observed (50.9% of the total amount was released after 15 days). This controlled release of EGF from nanofibers resulted in 43.6% higher proliferation of adipose-derived stem cells (ADSCs) on core–shell gelatin/PLLCL/EIF (cs) nanofibers than that on the blend gelatin/PLLCL/EIF (b) counterparts. Moreover, the rate of cell proliferation on gelatin/PLLCL/EIF (cs) and gelatin/PLLCL/EIF (b) from 5 to day 15 was 560% and 404%, respectively. Additionally, the researchers also noticed that the amount of differentiated epidermal cells on gelatin/PLLCL/EIF (cs) was superior to that observed on gelatin/PLLCL/EIF (b) membrane, 62.2% and 43.0%, respectively (as shown in Fig. 7).

4.2. Vitamins

The delivery of vitamins, particularly Vit-A, C and E to the wound site can improve the healing process [114,115]. Vit-A increases the number of macrophages and monocytes present at the wound site, stimulating the re-epithelialization and the collagen synthesis [116,117]. The antioxidant and anti-inflammatory activity, as well as the capacity to promote the angiogenesis and reduce scarring of Vit-E also contributes to enhance the wound healing [118]. An overview of different works reporting the incorporation of vitamins into electrospun nanofibers aimed for wound healing applications is shown in Table 5.

Taepaiboon et al. prepared CA solutions containing Vit-E (5 wt%) or Vit-A (0.5 wt%) that were used to produce nanofibrous membranes [119]. Their results revealed that the percentage of vitamins incorporated within the fiber mats was 83% and 45% for Vit-E and Vit-A, respectively. The incorporation of these molecules induced a decrease in the nanofibers mean diameter from 265 ± 39 nm (for CA nanofibers) to 253 ± 41 nm (for CA fibers containing Vit-E) and 247 ± 31 nm (for CA fibers containing Vit-A). Further, the release profile of vitamins from CA electrospun membranes in two different acetate buffer solutions (B/T medium (containing 0.5 vol% Tween 80) and B/T/M medium (containing 0.5 vol% Tween 80 and 10 vol% methanol)) was evaluated. The maximum release of Vit- E and Vit-A in B/T medium was ≈52% and ≈34% after 24 h, whereas when the sample was incubated in B/T/M medium this value increased to ≈ 95% and ≈ 96%, respectively. Sheng et al. explored the incorporation of a PEGylated derivative of Vit-E (TPGS) into SF nanofibers for enhancing the wound healing process [120]. To accomplish that, different blends containing TPGS (2, 4 and 8% w/w) and SF (25% w/v) were

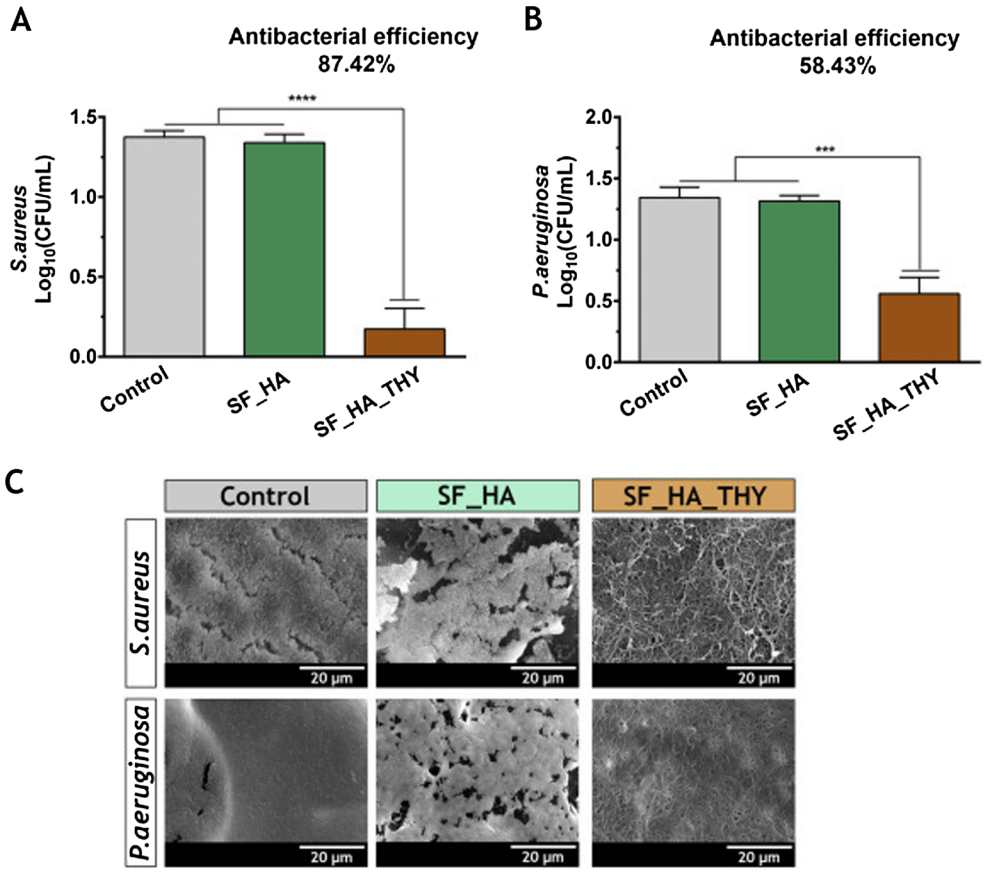

Fig. 5. Analysis of the antimicrobial activity exhibited by SF_HA and SF_HA_THY membranes against *S. aureus* (A) and *P. aeruginosa* (B). SEM images of control and nanofibrous membranes incubated with *S. aureus* and *P. aeruginosa*. Reproduced from [8] with permission from Elsevier.

electrospun. The produced membranes exhibited a burst release of TPGS, during the first 30 min, followed by a slow and controlled diffusion of this molecule over the following 72 h. Moreover, L929 cells remained viable and proliferated at the surface of TPGS loaded SF nanofibers.

In 2018, Kheradvar et al. reported the development of SF_PVA_AV nanofibers containing starch nanoparticles loaded with Vit-E (VE-SNPs) [121]. The produced VE-SNPs presented a round shape morphology, a mean diameter of 44.7 nm and an encapsulation efficiency of 91.63%. The SF_PVA_AV (40, 50, and 10 v/v%) nanofibers presented a mean fiber diameter of 298.23 ± 6.92 nm. These nanofibers displayed an initial rapid release of Vit-E within the first 4 h, followed by a sustained release over 144 h. Furthermore, the increased content of VE-SNPs loaded into the membranes resulted in a higher antioxidant activity (34.7 ± 2.05% (for 1 mg) and 66.27 ± 3.7% (for 5 mg)). On the other hand, *in vitro* assays also demonstrated the biocompatible profile of the electrospun membranes, since they were able to promote fibroblasts adhesion, spreading and proliferation.

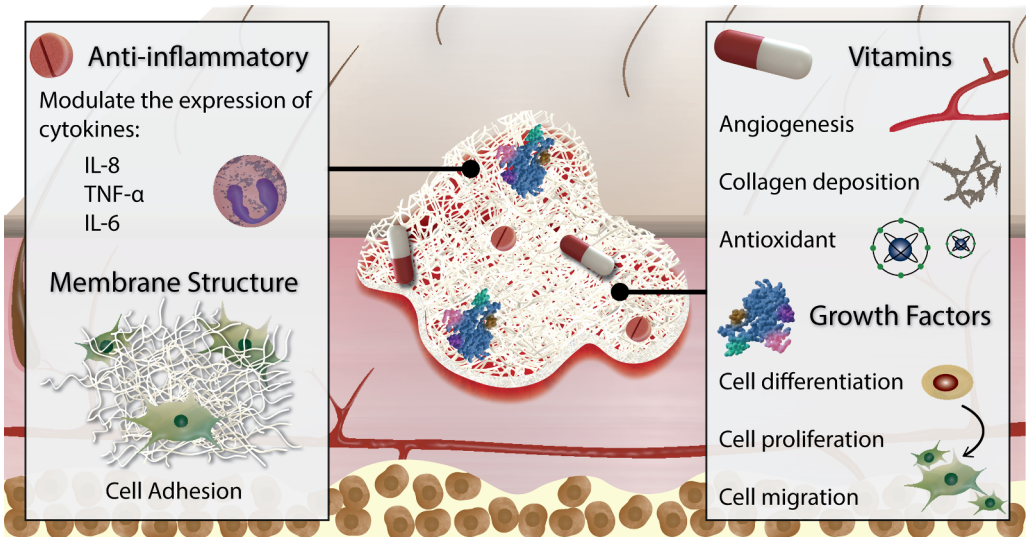

Fig. 6. Illustration of the different molecules that have been incorporated into electrospun nanofibers and their principal roles in the wound healing process.

Table 4
Examples of the growth factors incorporated into electrospun meshes to be used in wound management.

Growth factor	Polymer	Incorporation method	Fiber diameter	Release profile	Main Findings	Ref.
PDGF	CS/PEO/Fb	Blend electrospinning	- CS/PEO: 269.9 ± 68.4 nm - CS/PEO/Fb: 202.3 ± 113.2 nm	- Cumulative release of PDGF after 48 h of incubation was 1.8 ± 0.7, 4.4 ± 1.8, 11.4 ± 4.8 ng of PDGF/mL for initially incorporated concentrations of 2, 4, and 8 μg/mL.	- The sustained released of PDGF during 48 h promoted the fibroblast migration; - The dermal fibroblast migration was functionally equivalent to a single 50 ng/mL dose of PDGF.	[11]
rhEGF	PLGA/AV	Emulsion electrospinning	- PLGA: 561.61 ± 124.28 nm - PLGA/AV: 486.99 ± 114.73 nm - PLGA/AV/EGF: 356.03 ± 112.05 nm	- The release profile of rhEGF from nanofibers exhibited an initial burst release (35%) within the first 8 h, followed by a slower release phase (50%) up to 7 days.	- The cell proliferation in PLGA/AV/EGF nanofibers reached a threefold increase in comparison to the control; - *In vivo* assays showed that the animals treated with PLGA/AV/EGF and PLGA/AV nanofibers presented an increased reepithelization; - The PLGA/AV/EGF nanofibers decreased the duration of the inflammatory phase.	[81]
bFGF, EGF, VEGF and PDGF	- EGF: collagen - bFGF: HA - PDGF and VEGF:gelatin nanoparticles	Blend electrospinning	- Collagen nanofibres: 534 ± 128 nm - HA nanofibres: 486 ± 151 nm	- Gradual slow release for PDGF and VEGF from gelatin nanoparticles during 30 days; - bFGF was rapidly released from HA nanofibers, 90% in 5 days; - EGF was rapidly released from collagen nanofibers, 60% in 5 days.	- The initial release of bFGF and EGF mimicked the early stage of the wound healing process, while the slow controlled release of VEGF and PDGF imitated the late stage of skin regeneration; -*In vivo* assays demonstrated the capability of the nanofibers to promote the re-epithelialization, dermal reconstruction and vascularization in diabetic rats.	[101]
VEGF and PDGF	- VEGF: CS/PEO nanofibers - PDGF: PLGA nanoparticles	Blend electrospinning	- 1:1 CS/PEO: 116 ± 39 nm - 1:2 CS/PEO: 132 ± 39 nm	-The release profile of VEGF from nanofibers exhibited a burst release (63%) within 1 h. After 1 day, 100% of VEGF was released; - 28% of PDGF was released from PLGA nanoparticles at 2 h, followed by a sustained release (40%) for 7 days.	- The membranes loaded with GFs showed a faster cell growth (140.9 ± 0.8% for day 5 and 156.6 ± 6.6% for day 7) in comparison with control groups; - VEGF improved the angiogenesis, while PDGF enhanced the epithelium regeneration, collagen deposition and functional tissue remodelling.	[105]
PDGF	- Chitosan nanoparticles in PCL nanofibers	Blend electrospinning	- PCL: 0.76 ± 0.37 μm - PCL/NP:1.22 ± 0.78 μm - PCL/NP(PDGF): 1.21 ± 0.66 μm	- 12% of PDGF was released in first 24 h, following a sustained release during one week (about 83% of PDGF released).	- The released PDGF induced the cell alignment on nanofibrous matrix; - The expression of PDGFRβ gene was higher in cells seeded in contact with PCL/NP(PDGF) nanofibers; - The controlled release of PDGF had high potential to induce the proliferation and migration of fibroblast cells.	[110]
EGF, insulin, hydrocortisone, and retinoic acid	-Gelatin/PLLCL	- Blend electrospinning: gelatin/PLLCL (b) - Co-axial electrospinning: gelatin/PLLCL (cs)	- PLLCL: 456 ± 62 nm - Gelatin/PLLCL:382 ± 100 nm-gelatin/PLLCL/EIF (b): 299 ± 46 nm gelatin/PLLCL/EIF (cs): 366 ± 125 nm	- Gelatin/PLLCL/EIF (b): 77.8% of EGF released after 15 days; - Gelatin/PLLCL/EIF (cs): 50.9% of EGF released after 15 days.	- The cell proliferation of ADSCs was higher (43.6%) in gelatin/PLLCL/EIF (cs) than in gelatin/PLLCL/EIF (b); - The percentage of differentiated epidermal cells was 62.2% and 43.0% for gelatin/PLLCL/EIF (cs) and gelatin/PLLCL/EIF (b) membranes, respectively.	[111]
EGF	- PLGA/gelatin					[109]

(*continued on next page*)

Table 4 (*continued*)

Growth factor	Polymer	Incorporation method	Fiber diameter	Release profile	Main Findings	Ref.
		Emulsion electrospinning	- PLGA: 630 ± 80 nm - Gelatin: 175 ± 45 nm - PLGA/EGF/gelatin: 390 ± 75 nm	- The release profile of EGF exhibits a burst release (in first day), followed by a sustained release over 9 days (total release of EGF was 4.2 ± 0.2 ng/mL).	- The MTT assay revealed that the fibroblast proliferation was higher on PLGA/EGF/gelatin membranes; - The cell infiltration and the expression of collagen type I and III genes was also higher in EGF loaded nanofibers; - The PLGA/EGF/gelatin membranes also demonstrated auspicious blood clotting and platelet adhesion in comparison to the commercial wound dressing (Hansplast).	
	- PCL/HA	Emulsion electrospinning	- PCL: 272 ± 38 nm - PCL/HA: 184 ± 6 nm - PCL/HA/EGF: 149 ± 4.5 nm	- The EGF release profile exhibited an early burst release in 4 days (35 ± 1.5%); - The release profile of EGF stabilized over 25 days, reaching 43.5 ± 1.2%.	- The HA mediated increase of the membranes hydrophilicity promoted the release of EGF; - The release of EGF and HA promoted cell infiltration, regulate the collagen and TGF-β1 gene expression and increase the ratio of collagen III to collagen I; - PCL/HA/EGF membranes accelerated the epidermis regeneration in the early phases of wound healing; - The wounds treated with PCL/HA/EGF membranes presented a thicker and more organized epidermis layer in the early phases of wound healing.	[112]
bFGF and EGF	- PCL-PEG/PCL	- bFGF: coaxial electrospinning - VEGF:Chemical immobilization	Not available	- The release profile of bFGF displays an initial burst release, 30% of bFGF is released in the first 12 h; - The surface-immobilized EGF is scarcely released, less than 2% of immobilized EGF was released in 7 days.	- The nanofibrous membranes containing GFs promoted the wound healing process and improved re-epithelialization of wounded tissues; - The membranes increased the accumulation of collagen and matrix of keratin.	[113]

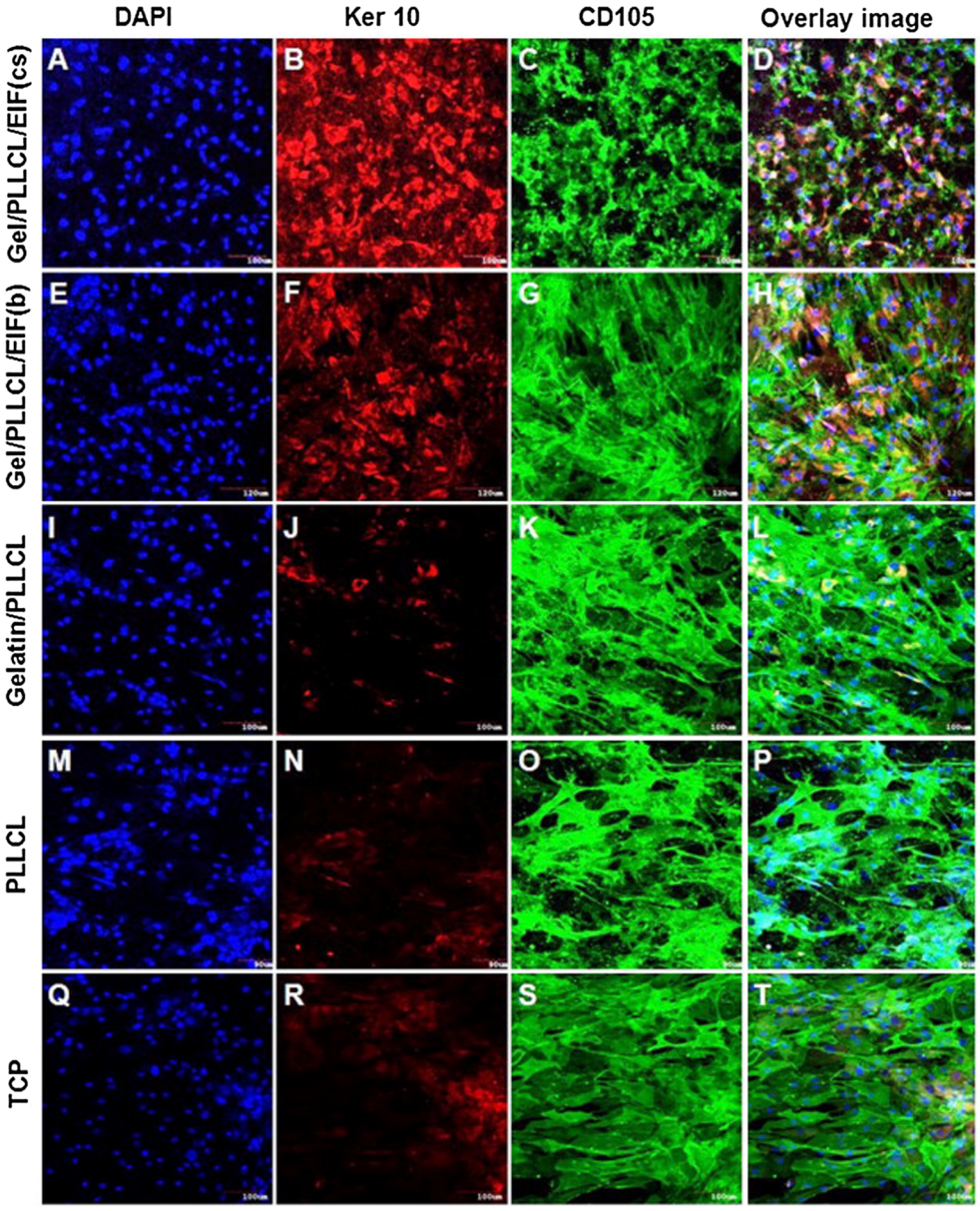

Fig. 7. Characterization of the adipose-derived stem cells (ADSCs) epidermal differentiation after 15 days of cells being seeded in contact with different materials. Dual immunocytochemical analysis of the expression of ker 10 (red channel) and CD 105 (green channel) on Gel/PLLCL/EIF (cs) (A-D); Gel/PLLCL/EIF (b) (E-H); Gelatin/PLLCL (I-L); PLLCL (M-P); and TCP (Q-T) at 20x magnification. Reproduced from [111] with permission from Elsevier. (For interpretation of the references to colour in this figure legend, the reader is referred to the web version of this article.)

Vit-C (or ascorbic acid) also plays an important role during the wound healing process, namely promotes the synthesis of collagen, encourages the keratinocytes differentiation and angiogenesis as well as provides protection against damages induced by UV radiation [122]. Moreover, the Vit-C deficiency leads to an impaired immune response and an increased susceptibility to wound infection [123]. Fan and their collaborators incorporated Vit-C into SF nanofibrous matrices [124]. Their results showed that the incorporation of Vit-C into SF nanofibers increased the fibers average diameter, from 362 ± 121 nm to 416 ± 133 nm (1 wt% Vit-C) and 506 ± 68 nm (for 3 wt% Vit-C). Further, the release profile of Vit-C from SF nanofibers displayed a burst release behaviour during the initial 20 min and then reached a plateau (≈60% for 1 wt% Vit-C and 70% for 3 wt% Vit-C) after 250 min. In addition, the incorporation of Vit-C into the membranes promoted higher cell viability and increased expression of some key functional genes (*Col1a1*, *Gpx1*, and *Cat*).

4.3. Molecules exhibiting anti-inflammatory activity

The inflammatory phase of the wound healing process begins almost simultaneously with the haemostasis, in order to prevent blood and fluid losses as well as to remove dead tissues and avoid infection [127,128]. In this phase, inflammatory cells (*i.e.* monocytes, macrophages, and neutrophils) play a crucial role in the wound cleansing, since they are responsible for removing all non-viable cells, bacteria-filled neutrophils, damaged ECM, and bacteria from the wound site. Moreover, these inflammatory cells are also involved in the production of GFs (like EGF, TGF-β, and FGF), that are responsible for attracting fibroblasts and smooth muscle cells into the wound [127]. However, when an exuberant and prolonged inflammatory process occurs, the continuous attraction of neutrophils and macrophages leads to the excessive production of inflammatory mediators, free radicals, and cytotoxic enzymes, which interrupt the physiological healing mechanisms and damage the surrounding tissue [12,129,130]. Therefore, the

Table 5
Examples of several vitamins that have been incorporated into electrospun nanofibers to improve the wound healing process.

Vitamins	Polymer	Incorporation method	Fiber diameter (nm)	EE (%)	Main conclusions	Refs.
Vit-A and Vit-E	Gelatin	Blend electrospinning	- Gelatin: 757 ± 161 nm - Gelatin loaded with Vitamins: 566 ± 163 nm	- Vit-E: 73.1 ± 3.2% - Vit- A: 71.4 ± 5.5%	- The gelatin nanofibers exhibited a sustained release of vitamins for more than 60 h; - The fibers promoted the adhesion and proliferation of L929 fibroblasts; - The Vit-E protected the Vit-A from oxidation process.	[100]
	CA	Blend electrospinning	- CA: 265 ± 39 nm - CA/Vit-E: 253 ± 41 nm - CA/ Vit-A: 247 ± 31 nm	- Vit-E: 83% - Vit-A: 45%	- In B/T medium, the maximum release of Vit- E at 24 h was ≈ 52%, whereas for Vit-A ≈ 34% was released at 6 h; - In B/T/M medium the maximum release of the Vit-E at 24 h was ≈ 95%, whereas for Vit-A 96% was released at 6 h.	[119]
Vit-E	SF	Blend electrospinning	- SF/Vit-E (2%): 722.52 ± 300 nm - SF/Vit-E (4%): 387.9 ± 114 nm - SF/Vit-E (8%): 384.3 ± 161 nm	- SF/Vit-E (2%): 65.82% - SF/Vit-E (4%): 78.59% - SF/Vit-E (8%): 70.02%	- The Vit-E displayed a burst release (during the first 30 min), followed a slow drug release over the subsequent 72 h; - The Vit-E loaded SF nanofibrous promoted the adhesion and proliferation of L929 cells; - The Vit-E loaded SF membranes were capable to protect the cells from damage induced by reactive oxygen species.	[120]
	SF/PVA/AV	Vit-E loaded into starch nanoparticles and blend with electrospinning solution	- SF/PVA/AV: 298.23 ± 6.92 nm	- Vit-E into startch nanoparticles: 91.63%	- The release profile of Vit-E consisted of an initial rapid release, followed by a slow release for 144 h; - The increase of Vit-E content resulted in higher antioxidant activity; - The fibroblasts cells remained viable, adhering and proliferating in contact with electrospun membranes.	[121]
Vit-C	CMCS/PEO	Blend electrospinning	- CMCS/PEO: 165 nm - CMSCS/PEO/PHT-Na: 125 nm	Not available	- The kinetics of drug release from the polymeric matrix was explained by the Fickian diffusion mechanism; - The membranes containing PHT-Na and Vit-C promoted a higher accumulation of stem cells (from 1.8×10^5 to 8.3×10^5 cells/mL).	[125]
	SF	Blend electrospinning	- SF: 362 ± 121 nm - SF/Vit-C (1%): 416 ± 133 nm - SF/Vit-C (3%): 506 ± 68 nm	Not available	- The release profile of Vit-C from SF nanofibers exhibited a burst peak during the initial 20 min; - The Vit-C promoted a higher fibroblast viability and increased the mRNA level of key functional genes (*Col1a1*, *Gpx1* and *Cat*).	[124]
	PLACL/ SF	Blend electrospinning	- PLACL/SF: 275 ± 50 nm - PLACL/SF/TCH/Vit-C: 265 ± 97 nm	Not available	- The PLACL/SF membrane had a water contact angle of 98 ± 1.2°, whereas the PLACL/SF/TCH/Vit-C showed 54 ± 2.5°; - An increased secretion of collagen was observed in the presence of nanofibers loaded with Vit-C; - The Vit-C promoted an augmented expression of F-actin.	[126]

Table 6
Description of some examples of electrospun membranes functionalized with anti-inflammatory molecules to improve the healing process.

Anti-inflammatory molecule	Polymer	Incorporation method	Fiber diameters	Release profile	Anti-inflammatory assay	Main findings	Refs.
Diclofenac (DLF)	DLF was incorporated into zein nanoparticles and posteriorly blend with PVA	Blend electrospinning	- PVA nanofibers: 202.41 ± 25.54 nm - PVA/zein NPs: 311.18 ± 45.56 nm - PVA/zein NPs-DLF: 324.42 ± 72.80 nm	- In the first stage, 36% of DLF was released from NPs after 8 h; - The release profile of DLF reached a plateau after 3 days, in which 80% of the drug was released.	Not available	- The NPs were well dispersed and distributed uniformly within nanofibers; - The membrane was biocompatible in contact with fibroblasts, improving its proliferation and spreading.	[20]
Ibuprofen	PLA	Blend electrospinning	- PLA/IBP (10%): 329.11 ± 249.62 nm - PLA/IBP (20%): 478.31 ± 167.61 nm - PLA/IBP(30%): 585.38 ± 131.51 nm	- 0.25 mg of IBP released from PLA/IBP (30%) nanofibers after 336 h.	Not available	-The greatest cell viability and proliferation was recorded in nanofibers containing 20 wt% IBP; - The incorporation of IBP into PLA nanofibers promoted an increased viability and proliferation of both HEK and HDF.	[140]
Ketoprofen	PCL/gelatin	Emulsion electrospining	- PCL/ketoprofen: 345 nm - PCL/gelatin/ketoprofen: 272 nm	- PCL/ketoprofen: initial burst release profile that reached a plateau (90%) after 12 min; - PCL/gelatin/Ketoprofen: continuous and sustained release for 4 days.	Not available	- Ketoprofen-containing electrospun membranes are biocompatible in contact with L929 mouse fibroblast cells; - The cell growth was 1.93 and 3.07 times higher in PCL/gelatin nanofibers in comparison with PCL membranes and TCPS plate, respectively.	[144]
Polypropylene fumarate (PPF)	POCA	Blend electrospinning	- POCA/PDF: 0.8 ± 0.1 μm	Not available	- IL-6 and IL-1β expression was 4 and 24 times inferior in POCA/PDF electrospun membranes group; - MPO values and the inflammation process decreased (skin thickness:14.3 ± 2.5 μm), when the burn was covered with POCA/PDF dressing.	- The presence of fumarate reduces the cytokines and neutrophils production; - The skin treated with POCA:PDF membranes exhibited a thin epidermal layer and low number of inflammatory cells.	[145]
Curcumin	PCL	Blend electrospinning	- PCL:range 300–400 nm - PCL/curcumin: 200–800 nm	- PCL/curcumin (17%): 35 μg was released at 3 day; - PCL/curcumin (3%): 20 μg was released at 3 day.	- The IL-6 release decreased in the PCL/curcumin (7%) nanofibers group.	- The ORAC assay also demonstrated the anti-oxidant properties of curcumin-loaded fibers; - The membranes were biocompatible and displayed a cytoprotective effect towards human fibroblasts cells; - *In vivo* assays demonstrated the ability of PCL/curcumin nanofibers to improve the rate of wound closure in a diabetic mouse model.	[135]
Naproxen (NAP)	Cellulose acetate (CA)	-Blend electrospinning: CA/NAP (NF-1) -Co-axial electrospinning:core (NAP/CA) and sheath (CA) (NF-2); core (NAP loaded liposomes and sodium hyaluronate) and sheath (CA) (NF-3)	- NF-1: 409.3 ± 152.5 nm - NF-2: 419.2 ± 178.2 nm - NF-3: 359.4 ± 126.2 nm	- NF-1: 90.9% of NAP is released in 8 h; - NF-2: 80.3% of NAP is released in 8 h; - NF-3: 47.1% of NAP is released within 8 h, following a slow and sustained release for 12 days.	Not available	- The drug release from NF-1 and NF-2 nanofibers occur by a non-Fickian diffusion mechanism; - In NF-3 nanofibers, the drug release shows specific behaviour, in which a burst release occurs in first 8 h, and then a sustained drug release occurs for the following 12 days.	[146]

(*continued on next page*)

Table 6 (*continued*)

Anti-inflammatory molecule	Polymer	Incorporation method	Fiber diameters	Release profile	Anti-inflammatory assay	Main findings	Refs.
Chrysin (Chr)	PCL/PEG	Blend electrospinning	- PCL/PEG: 300–400 nm - PCL/PEG/Chr: 250–650 nm	- PCL/PEG/Chr (5%): 25 μg of Chr was released after 3 days; - PCL/PEG/Chr (15%): %): 43 μg of Chr was released after 3 days.	- The macrophages incubated with PCL/PEG/Chr (15%) presented a 67%, 52% and 72% reduction in the Il-6, Il-1β and TNF-α expression, respectively; - The cells NO production decreased with the Chr content, 16.22 μM and 14.60 μM for PCL/PEG/Chr (5%) and (15%), respectively.	- The nanofibers were biocompatible and exhibited anti-oxidant activity; - The cytoprotective effect of Chr-loaded nanofibrous membranes towards human fibroblast cells was also demonstrated; - The anti-inflammatory capability of Chr-loaded nanofibrous mats was evidenced by the macrophages decreased expression of IL-6, IL-1β, TNF-α and NO.	[143]
Montelukast	PMVEMA/PLGA	Blend electrospinning	- PMVEMA/PLGA/Montelukast: 101.1–283 nm	- The cumulative drug release was faster on the increased amount of montekulast.	Not available	- The addition of the montekulast into PMVEMA/PLGA nanofibers did elicit any cytotoxicity effect, allowing the cells adhesion and proliferation; - The nanofibers promoted an increased platelet adhesion in comparison to the negative control.	[147]
Dexamethasone	SF/PEO SF/PEO/DEX1 (1 mg/mL) SF/PEO/DEX2 (2 mg/mL)	Blend and Emulsion electrospinning	- SF/PEO: 446.25 ± 113.93 nm - SF/PEO/DEX1: 511.11 ± 109.03 nm - SF/PEO/DEX2: 528.50 ± 148.00 nm	- Using blend electrospinning: the release of Dex from SF/PEO/Dex2 was 30% in the first 2 h and 8% after 24 h; - Using emulsion electrospinning: the release of Dex from SF/PEO/Dex2 was 21% in the first 2 h and 42% after 24 h.	- The release Dex can reduce PIECs inflammatory damage, which was induced by LPS.	- Core-shell structure provided a slow release of drug from nanofibers; - The incorporation of Dex provided a protective effect to the nanofibers on PIECS damaged by LPS.	[148]

incorporation of anti-inflammatory molecules into wound dressings is a key approach for the treatment of skin injuries, since these molecules are capable of inhibiting the development of chronic inflammation and to avoid the accumulation of free radicals [14,19,131]. In Table 6 examples of different anti-inflammatory molecules that have been incorporated into electrospun membranes aimed to be applied as wound dressings are provided.

Among the different molecules used, curcumin was one of the first anti-inflammatory agents incorporated into electrospun nanofibers [132]. Curcumin is able to decrease the release of inflammatory cytokines from monocytes and macrophages (interleukin (IL)-8 and tumour necrosis factor (TNF)-α) as well as inhibit the enzymes associated with inflammation (*cyclo*-oxygenase (COX)-2 and lipoxygenase (LOX)) [133,134]. Merrell et al. developed PCL nanofibers loaded with curcumin for being applied as wound dressings [135]. Their results showed that the incorporation of curcumin (3 and 17% w/w) changed the nanofibers size diameter distribution from 300 to 400 nm (for PCL nanofibers) to 200–800 nm (for PCL/curcumin nanofibers). Moreover, the produced nanofibers performed the release of curcumin for 3 days, prompting a cytoprotective effect on HFF-1 cells, when they were incubated with hydrogen peroxide. Further, the curcumin-loaded PCL nanofibrous mats reduced the pro-inflammatory response of mouse peritoneal macrophages stimulated with lipopolysaccharide (LPS). The expression of IL-6 was reduced from ≈1220 pg/mL on the cells treated with PCL nanofibers to ≈600 pg/mL and 400 pg/mL for the cells treated with PCL fibers containing 3% and 17% of curcumin, respectively. Additionally, the animals treated with curcumin-loaded PCL nanofibers showed almost 80% of wound closure at day 10, contrasting with the 60% registered for mice treated with PCL nanofibers.

Nonsteroidal anti-inflammatory drugs (NSAID) are another type of molecules that are usually used to treat inflammation as well as control pain and fever [136]. Among them, the application of ibuprofen (IBP) has been widely reported, however, the continued oral administration or large doses of IBP may have associated side effects, such as kidney damage and gastric ulcers. Therefore, the topical administration of IBP may have a positive impact on the treatment of skin injuries [137–139]. Mohiti-Asli et al. incorporated IBP into PLA nanofibers for promoting the regeneration of full thickness wounds [140]. The incorporation of IBP resulted in the production of nanofibers with higher fiber diameters, *i.e.* 10%, 20% and 30% of IBP-loaded nanofibers displayed a diameter of 329.11 ± 249.62 nm, 478.31 ± 167.61 nm, and 585.38 ± 131.51 nm, respectively. Moreover, these nanofibrous mats were able to support the cell adhesion and proliferation, particularly the PLA nanofibrous mat with 20% of IBP. The authors also observed that the PLA nanofibrous mat containing 20% of IBP could be degraded when applied in full-thickness wounds in mice, supporting simultaneously the wound closure (60% wound contraction after 14 days).

Chrysin (Chr), a natural flavonoid present in various plant extracts, has also been incorporated into nanofiber based wound dressings due to its anti-inflammatory properties [141,142]. The Chr suppresses the lipopolysaccharide-induced COX-2 expression, inhibits the nitric oxide (NO) synthase as well as the release of NO and pro-inflammatory cytokines such as TNF-α and IL-1β. Deldar and coworkers incorporated Chr into PCL/poly(ethylene glycol) (PEG) nanofibrous membranes to produce a wound dressing that displays antioxidant and anti-inflammatory activities [143]. The inclusion of Chr, at 5 or 15 wt%, into PCL/PEG nanofibers changed the nanofibers diameter distribution from 300 to 400 nm (PCL/PEG membranes) to 250–650 nm (PCL/PEG/Chr membranes). Further, the Chr was released from the nanofibers in a sustained manner over 72 h, independently of the loaded amount. This behaviour resulted in the reduction of the expression of pro-inflammatory cytokines in 67%, 52% and 72% for IL-6, IL-1β, and TNF-α, respectively, when J774A1 cells were in contact with PCL/PEG nanofibrous membranes loaded with Chr 15% (w/w). Additionally, a decrease on the NO production by macrophage cells was also noticed from 29.53 μM to 15.50 μM (for PCL/PEG/Chr 5% nanofibers) and to 12.52 μM (for PCL/PEG/Chr 15% nanofibers). Such results supported the Chr-loaded PCL/PEG nanofibrous membranes capacity to inhibit the inflammatory process.

5. Conclusions and future perspectives

The wound healing is considered one of the most complex processes that occur in the human body since it plays an important role in the maintenance of the body homeostasis. Up to now, researchers have been developing different types of wound dressings such as hydrogels, sponges, films and membranes to improve the healing process. Amidst them, the electrospun membranes have been the target of a wide number of works due to the structural similarity with the skin ECM, high surface area-volume ratio, porosity, and capacity to act as a drug delivery system. Furthermore, electrospun membranes also support cell adhesion, proliferation, and differentiation as well as act as a barrier for preventing the occurrence and establishment of infections. Additionally, the incorporation of molecules (*e.g.* antibiotics, silver-based materials, molecules from natural extracts (*e.g.* essential oils, chitosan, Aloe vera, etc), GFs, vitamins, and anti-inflammatory molecules) into electrospun membranes and its topical administration at the wound site has been explored to avoid/impair the skin infections and mediate the different phases of the healing process towards a more effective skin regeneration.

Nevertheless, despite the encouraging results obtained in recent studies in the enhancement of skin regeneration, there are still several challenges for the translation of nanofibers into practical healthcare applications. For example, nanofibers orientation, arrangement, and porosity need to be carefully controlled since these factors will influence the biological performance of the nanofibers (such as biomolecules adsorption, cell adhesion, and proliferation). Additionally, when different biomolecules are loaded within nanofibers several key factors must be optimized in order to eliminate their burst release, overcome the low delivery efficiency and manipulate the multi-stage delivery of different biomolecules within the same nanofibrous membrane.

In the near future, the combination between the different nanofiber production techniques and surface modification methodologies, such as heat and plasma treatment will allow the improvement of the nanofiber's physiochemical properties. Moreover, the development of pH, temperature, light, electrical or magnetic field responsive nanofibers will provide a controlled or multi-stage release of the biological molecules at the wound site. Finally, the realization of clinical trials is fundamental for the commercialization of electrospun membranes-based drug delivery systems aimed for skin regeneration as well as contribute to enhance patient's quality of life.

Acknowledgments

Authors would like to acknowledge the financial support from FEDER funds through the POCI—COMPETE 2020—Operational Programme Competitiveness and Internationalization in Axis I—Strengthening research, technological development and innovation (Project POCI-01-0145-FEDER- 007491) and National Funds by FCT—Foundation for Science and Technology (Project UID/Multi/00709/2013). Sónia P. Miguel and André F. Moreira acknowledge their Ph.D. fellowships from FCT (SFRH/BD/109563/2015 and SFRH/BD/109482/2015, respectively).

References

[1] J.S. Boateng, K.H. Matthews, H.N. Stevens, G.M. Eccleston, Wound healing dressings and drug delivery systems: a review, J. Pharm. Sci. 97 (2008) 2892–2923.
[2] S. Dhivya, V.V. Padma, E. Santhini, Wound dressings–a review, BioMedicine 5 (2015) 22.
[3] S.P. Miguel, M.P. Ribeiro, H. Brancal, P. Coutinho, I.J. Correia, Thermoresponsive chitosan–agarose hydrogel for skin regeneration, Carbohydr. Polym. 111 (2014) 366–373.

[4] M.K. Strecker-McGraw, T.R. Jones, D.G. Baer, Soft tissue wounds and principles of healing, Emerg. Med. Clin. North Am. 25 (2007) 1–22.
[5] D. Sundaramurthi, U.M. Krishnan, S. Sethuraman, Electrospun nanofibers as scaffolds for skin tissue engineering, Polym. Rev. 54 (2014) 348–376.
[6] W.E. Teo, W. He, S. Ramakrishna, Electrospun scaffold tailored for tissue-specific extracellular matrix, Biotechnol. J.: Healthcare Nutri. Technol. 1 (2006) 918–929.
[7] S.P. Miguel, M.P. Ribeiro, P. Coutinho, I.J. Correia, Electrospun polycaprolactone/aloe vera_chitosan nanofibrous asymmetric membranes aimed for wound healing applications, Polymers 9 (2017) 183.
[8] S.P. Miguel, D. Simões, A.F. Moreira, R.S. Sequeira, I.J. Correia, Production and characterization of electrospun silk fibroin based asymmetric membranes for wound dressing applications, Int. J. Biol. Macromol. 121 (2018) 524–535.
[9] Y. Ding, W. Li, F. Zhang, Z. Liu, N. Zanjanizadeh Ezazi, D. Liu, H.A. Santos, Electrospun fibrous architectures for drug delivery, tissue engineering and cancer therapy, Adv. Funct. Mater. (2018).
[10] T.J. Sill, H.A. von Recum, Electrospinning: applications in drug delivery and tissue engineering, Biomaterials 29 (2008) 1989–2006.
[11] T.T. Yuan, A.M.D. Foushee, M.C. Johnson, A.R. Jockheck-Clark, J.M. Stahl, Development of electrospun chitosan-polyethylene oxide/fibrinogen biocomposite for potential wound healing applications, Nanoscale Res. Lett. 13 (2018) 88.
[12] M. Abrigo, S.L. McArthur, P. Kingshott, Electrospun nanofibers as dressings for chronic wound care: advances, challenges, and future prospects, Macromol. Biosci. 14 (2014) 772–792.
[13] V. Leung, F. Ko, Biomedical applications of nanofibers, Polym. Adv. Technol. 22 (2011) 350–365.
[14] J. Boateng, O. Catanzano, Advanced therapeutic dressings for effective wound healing—a review, J. Pharm. Sci. 104 (2015) 3653–3680.
[15] S.P. Miguel, D.R. Figueira, D. Simões, M.P. Ribeiro, P. Coutinho, P. Ferreira, I.J. Correia, Electrospun polymeric nanofibres as wound dressings: a review, Colloids Surf., B 169 (2018) 60–71.
[16] S.-F. Chou, D. Carson, K.A. Woodrow, Current strategies for sustaining drug release from electrospun nanofibers, J. Contr. Rel. 220 (2015) 584–591.
[17] L. Preem, K. Kogermann, Electrospun Antimicrobial Wound Dressings: Novel Strategies to Fight Against Wound Infections, in: C. Springer (Ed.) Recent Clinical Techniques, Results, and Research in Wounds; 2018.
[18] H. Cheng, X. Yang, X. Che, M. Yang, G. Zhai, Biomedical application and controlled drug release of electrospun fibrous materials, Mater. Sci. Eng. C Mater. Biol. Appl. 90 (2018) 750–763.
[19] P.I. Morgado, S.P. Miguel, I.J. Correia, A. Aguiar-Ricardo, Ibuprofen loaded PVA/chitosan membranes: a highly efficient strategy towards an improved skin wound healing, Carbohydr. Polym. 159 (2017) 136–145.
[20] S. Ghalei, H. Asadi, B. Ghalei, Zein nanoparticle-embedded electrospun PVA nanofibers as wound dressing for topical delivery of anti-inflammatory diclofenac, J. Appl. Polym. Sci. 135 (2018) 46643.
[21] R.F. Pereira, C.C. Barrias, P.L. Granja, P.J. Bartolo, Advanced biofabrication strategies for skin regeneration and repair, Nanomedicine 8 (2013) 603–621.
[22] D.I. Braghirolli, D. Steffens, P. Pranke, Electrospinning for regenerative medicine: a review of the main topics, Drug Discov. Today 19 (2014) 743–753.
[23] S.S. Ray, S.-S. Chen, C.-W. Li, N.C. Nguyen, H.T. Nguyen, A comprehensive review: electrospinning technique for fabrication and surface modification of membranes for water treatment application, RSC Adv. 6 (2016) 85495–85514.
[24] X. Hu, S. Liu, G. Zhou, Y. Huang, Z. Xie, X. Jing, Electrospinning of polymeric nanofibers for drug delivery applications, J. Contr. Rel. 185 (2014) 12–21.
[25] A. Balaji, M. Vellayappan, A. John, A. Subramanian, S. Jaganathan, E. Supriyanto, S. Razak, An insight on electrospun-nanofibers-inspired modern drug delivery system in the treatment of deadly cancers, RSC Adv. 5 (2015) 57984–58004.
[26] J.S. Im, J. Yun, Y.-M. Lim, H.-I. Kim, Y.-S. Lee, Fluorination of electrospun hydrogel fibers for a controlled release drug delivery system, Acta Biomater. 6 (2010) 102–109.
[27] A. Saraf, L.S. Baggett, R.M. Raphael, F.K. Kasper, A.G. Mikos, Regulated non-viral gene delivery from coaxial electrospun fiber mesh scaffolds, J. Contr. Rel. 143 (2010) 95–103.
[28] M. Zamani, M.P. Prabhakaran, S. Ramakrishna, Advances in drug delivery via electrospun and electrosprayed nanomaterials, Int. J. Nanomed. 8 (2013) 2997.
[29] M. Grassi, G. Grassi, Mathematical modelling and controlled drug delivery: matrix systems, Curr. Drug Deliv. 2 (2005) 97–116.
[30] W. Ji, Y. Sun, F. Yang, J.J. van den Beucken, M. Fan, Z. Chen, J.A. Jansen, Bioactive electrospun scaffolds delivering growth factors and genes for tissue engineering applications, Pharm. Res. 28 (2011) 1259–1272.
[31] G. Han, R. Ceilley, Chronic wound healing: a review of current management and treatments, Adv. Therapy 34 (2017) 599–610.
[32] A.R. Siddiqui, J.M. Bernstein, Chronic wound infection: facts and controversies, Clin. Dermatol. 28 (2010) 519–526.
[33] C. Dhand, M. Venkatesh, V.A. Barathi, S. Harini, S. Bairagi, E.G.T. Leng, N. Muruganandham, K.Z.W. Low, M.H.U.T. Fazil, X.J. Loh, Bio-inspired cross-linking and matrix-drug interactions for advanced wound dressings with long-term antimicrobial activity, Biomaterials 138 (2017) 153–168.
[34] M. Yazdanbakhsh, A. Rashidi, M. Rahimi, R. Khajavi, H. Shafaroodi, The effect of impregnated alpha-cellulose nanofibers with ciprofloxacin hydrochloride on staphylococcus aureus in vitro and healing process of wound in rat, Regener. Eng. Transl. Med. 4 (2018) 247–256.
[35] M. Ceylan, S.-Y. Yang, R. Asmatulu, Effects of gentamicin-loaded PCL nanofibers on growth of gram positive and gram negative bacteria, Int. J. Appl. Microbiol. Biotechnol. Res. 5 (2017) 40–51.
[36] A.C. Alavarse, F.W. de Oliveira Silva, J.T. Colque, V.M. da Silva, T. Prieto, E.C. Venancio, J.-J. Bonvent, Tetracycline hydrochloride-loaded electrospun nanofibers mats based on PVA and chitosan for wound dressing, Mater. Sci. Engng. C 77 (2017) 271–281.
[37] D. Semnani, N. Poursharifi, N. Banitaba, A. Fakhrali, Electrospun polyvinylidene pyrolidone/gelatin membrane impregnated with silver sulfadiazine as wound dressing for burn treatment, Bull. Mater. Sci. 41 (2018) 72.
[38] S. Torres-Giner, A. Martinez-Abad, J.V. Gimeno-Alcañiz, M.J. Ocio, J.M. Lagaron, Controlled delivery of gentamicin antibiotic from bioactive electrospun polylactide-based ultrathin fibers, Adv. Eng. Mater. 14 (2012) B112–B122.
[39] H. Li, G.R. Williams, J. Wu, Y. Lv, X. Sun, H. Wu, L.-M. Zhu, Thermosensitive nanofibers loaded with ciprofloxacin as antibacterial wound dressing materials, Int. J. Pharm. 517 (2017) 135–147.
[40] M. Mohseni, A. Shamloo, Z. Aghababaei, M. Vossoughi, H. Moravvej, Antimicrobial wound dressing containing silver sulfadiazine with high biocompatibility: in vitro study, Artif. Organs 40 (2016) 765–773.
[41] S. Ranghar, P. Sirohi, P. Verma, V. Agarwal, Nanoparticle-based drug delivery systems: promising approaches against infections, Brazil. Archiv. Biol. Technol. 57 (2014) 209–222.
[42] N. Alhusein, I.S. Blagbrough, M.L. Beeton, A. Bolhuis, A. Paul, Electrospun zein/PCL fibrous matrices release tetracycline in a controlled manner, killing *Staphylococcus aureus* both in biofilms and ex vivo on pig skin, and are compatible with human skin cells, Pharm. Res. 33 (2016) 237–246.
[43] N. Monteiro, M. Martins, A. Martins, N.A. Fonseca, J.N. Moreira, R.L. Reis, N.M. Neves, Antibacterial activity of chitosan nanofiber meshes with liposomes immobilized releasing gentamicin, Acta Biomater. 18 (2015) 196–205.
[44] X. Liu, L.H. Nielsen, S.N. Kłodzińska, H.M. Nielsen, H. Qu, L.P. Christensen, J. Rantanen, M. Yang, Ciprofloxacin-loaded sodium alginate/poly (lactic-co-glycolic acid) electrospun fibrous mats for wound healing, Eur. J. Pharm. Biopharm. 123 (2018) 42–49.
[45] L. Wilkinson, R. White, J. Chipman, Silver and nanoparticles of silver in wound dressings: a review of efficacy and safety, J. Wound Care 20 (2011) 543–549.
[46] J. Song, N.L. Birbach, J.P. Hinestroza, Deposition of silver nanoparticles on cellulosic fibers via stabilization of carboxymethyl groups, Cellulose 19 (2012) 411–424.
[47] J. Tian, K.K. Wong, C.M. Ho, C.N. Lok, W.Y. Yu, C.M. Che, J.F. Chiu, P.K. Tam, Topical delivery of silver nanoparticles promotes wound healing, ChemMedChem: Chem. Enab. Drug Discov. 2 (2007) 129–136.
[48] T.C. Dakal, A. Kumar, R.S. Majumdar, V. Yadav, Mechanistic basis of antimicrobial actions of silver nanoparticles, Front. Microbiol. 7 (2016) 1831.
[49] S. Zhang, Y. Tang, B. Vlahovic, A review on preparation and applications of silver-containing nanofibers, Nanoscale Res. Lett. 11 (2016) 80.
[50] K.R. Aadil, S.I. Mussatto, H. Jha, Synthesis and characterization of silver nanoparticles loaded poly (vinyl alcohol)-lignin electrospun nanofibers and their antimicrobial activity, Int. J. Biol. Macromol. 120 (2018) 763–767.
[51] K.R. Aadil, A. Barapatre, A.S. Meena, H. Jha, Hydrogen peroxide sensing and cytotoxicity activity of Acacia lignin stabilized silver nanoparticles, Int. J. Biol. Macromol. 82 (2016) 39–47.
[52] K.R. Aadil, D. Prajapati, H. Jha, Improvement of physcio-chemical and functional properties of alginate film by Acacia lignin, Food Pack. Shelf Life 10 (2016) 25–33.
[53] H. Dong, D. Wang, G. Sun, J.P. Hinestroza, Assembly of metal nanoparticles on electrospun nylon 6 nanofibers by control of interfacial hydrogen-bonding interactions, Chem. Mater. 20 (2008) 6627–6632.
[54] F.G. Santos, L.C. Bonkovoski, F.P. Garcia, T.S. Cellet, M.A. Witt, C.V. Nakamura, A.F. Rubira, E.C. Muniz, Antibacterial performance of a PCL–PDMAEMA blend nanofiber-based scaffold enhanced with immobilized silver nanoparticles, ACS Appl. Mater. Interfaces 9 (2017) 9304–9314.
[55] S.J. Lee, D.N. Heo, J.-H. Moon, W.-K. Ko, J.B. Lee, M.S. Bae, S.W. Park, J.E. Kim, D.H. Lee, E.-C. Kim, Electrospun chitosan nanofibers with controlled levels of silver nanoparticles preparation, characterization and antibacterial activity, Carbohydr. Polym. 111 (2014) 530–537.
[56] M. Akter, M.T. Sikder, M.M. Rahman, A.A. Ullah, K.F.B. Hossain, S. Banik, T. Hosokawa, T. Saito, M. Kurasaki, A systematic review on silver nanoparticles-induced cytotoxicity: physicochemical properties and perspectives, J. Adv. Res. 9 (2017) 1–16.
[57] Y.K. Tak, S. Pal, P.K. Naoghare, S. Rangasamy, J.M. Song, Shape-dependent skin penetration of silver nanoparticles: does it really matter? Sci. Rep. 5 (2015) 16908.
[58] F.L. Filon, D. Bello, J.W. Cherrie, A. Sleeuwenhoek, S. Spaan, D.H. Brouwer, Occupational dermal exposure to nanoparticles and nano-enabled products: Part I—factors affecting skin absorption, Int. J. Hyg. Environ. Health 219 (2016) 536–544.
[59] M. Wang, X. Lai, L. Shao, L. Li, Evaluation of immunoresponses and cytotoxicity from skin exposure to metallic nanoparticles, Int. J. Nanomed. 13 (2018) 4445.
[60] M.M. Sufian, J.Z.K. Khattak, S. Yousaf, M.S. Rana, Safety issues associated with the use of nanoparticles in human body, Photodiagn. Photodyn. Ther. 19 (2017) 67–72.
[61] W. Ge, Y. Zhao, F.-N. Lai, J.-C. Liu, Y.-C. Sun, J.-J. Wang, S.-F. Cheng, X.-F. Zhang, L.-L. Sun, L. Li, Cutaneous applied nano-ZnO reduce the ability of hair follicle stem cells to differentiate, Nanotoxicology 11 (2017) 465–474.
[62] V. Sharma, S.K. Singh, D. Anderson, D.J. Tobin, A. Dhawan, Zinc oxide nanoparticle induced genotoxicity in primary human epidermal keratinocytes, J. Nanosci. Nanotechnol. 11 (2011) 3782–3788.
[63] G. Rath, T. Hussain, G. Chauhan, T. Garg, A.K. Goyal, Collagen nanofiber containing silver nanoparticles for improved wound-healing applications, J. Drug Target. 24 (2016) 520–529.
[64] Y. Liu, Y. Liu, N. Liao, F. Cui, M. Park, H.-Y. Kim, Fabrication and durable antibacterial properties of electrospun chitosan nanofibers with silver nanoparticles, Int. J. Biol. Macromol. 79 (2015) 638–643.

[65] C. Li, R. Fu, C. Yu, Z. Li, H. Guan, D. Hu, D. Zhao, L. Lu, Silver nanoparticle/chitosan oligosaccharide/poly (vinyl alcohol) nanofibers as wound dressings: a preclinical study, Int. J. Nanomed. 8 (2013) 4131.
[66] X. Wang, F. Cheng, J. Gao, L. Wang, Antibacterial wound dressing from chitosan/polyethylene oxide nanofibers mats embedded with silver nanoparticles, J. Biomater. Appl. 29 (2015) 1086–1095.
[67] S. Burt, Essential oils: their antibacterial properties and potential applications in foods—a review, Int. J. Food Microbiol. 94 (2004) 223–253.
[68] A. Brochot, A. Guilbot, L. Haddioui, C. Roques, Antibacterial, antifungal, and antiviral effects of three essential oil blends, MicrobiologyOpen 6 (2017) e00459.
[69] R.G. Bachir, M. Benali, Antibacterial activity of the essential oils from the leaves of Eucalyptus globulus against *Escherichia coli* and *Staphylococcus aureus*, Asian Pacific J. Trop. Biomed. 2 (2012) 739–742.
[70] Q. Liu, X. Meng, Y. Li, C.-N. Zhao, G.-Y. Tang, H.-B. Li, Antibacterial and antifungal activities of spices, Int. J. Mol. Sci. 18 (2017) 1283.
[71] S. Chouhan, K. Sharma, S. Guleria, Antimicrobial activity of some essential oils—present status and future perspectives, Medicines 4 (2017) 58.
[72] M.S. Akthar, B. Degaga, T. Azam, Antimicrobial activity of essential oils extracted from medicinal plants against the pathogenic microorganisms: a review, J. Issues ISSN 2350 (2014) 1588.
[73] A.R. Koroch, H.R. Juliani, J.A. Zygadlo, Bioactivity of essential oils and their components, Flavours and fragrances, Springer, 2007, pp. 87–115.
[74] V.K. Bajpai, A. Sharma, K.-H. Baek, Antibacterial mode of action of *Cudrania tricuspidata* fruit essential oil, affecting membrane permeability and surface characteristics of food-borne pathogens, Food Control 32 (2013) 582–590.
[75] F. Lv, H. Liang, Q. Yuan, C. Li, In vitro antimicrobial effects and mechanism of action of selected plant essential oil combinations against four food-related microorganisms, Food Res. Int. 44 (2011) 3057–3064.
[76] D. Simões, S.P. Miguel, M.P. Ribeiro, P. Coutinho, A.G. Mendonça, I.J. Correia, Recent advances on antimicrobial wound dressing: a review, Eur. J. Pharm. Biopharm. 127 (2018) 130–141.
[77] I. Liakos, L. Rizzello, H. Hajiali, V. Brunetti, R. Carzino, P. Pompa, A. Athanassiou, E. Mele, Fibrous wound dressings encapsulating essential oils as natural antimicrobial agents, J. Mater. Chem. B 3 (2015) 1583–1589.
[78] A.H. Banskota, Y. Tezuka, S. Kadota, Recent progress in pharmacological research of propolis, Phytother. Res. 15 (2001) 561–571.
[79] J.I. Kim, H.R. Pant, H.-J. Sim, K.M. Lee, C.S. Kim, Electrospun propolis/polyurethane composite nanofibers for biomedical applications, Mater. Sci. Eng., C 44 (2014) 52–57.
[80] F. Croisier, P. Sibret, C.C. Dupont-Gillain, M.J. Genet, C. Detrembleur, C. Jérôme, Chitosan-coated electrospun nanofibers with antibacterial activity, J. Mater. Chem. B 3 (2015) 3508–3517.
[81] I. Garcia-Orue, G. Gainza, F.B. Gutierrez, J.J. Aguirre, C. Evora, J.L. Pedraz, R.M. Hernandez, A. Delgado, M. Igartua, Novel nanofibrous dressings containing rhEGF and aloe vera for wound healing applications, Int. J. Pharm. 523 (2017) 556–566.
[82] J. Hamman, Composition and applications of aloe vera leaf gel, Molecules 13 (2008) 1599–1616.
[83] K. Eshun, Q. He, Aloe vera: a valuable ingredient for the food, pharmaceutical and cosmetic industries—a review, Crit. Rev. Food Sci. Nutr. 44 (2004) 91–96.
[84] F.L. Mi, Y.B. Wu, S.S. Shyu, J.Y. Schoung, Y.B. Huang, Y.H. Tsai, J.Y. Hao, Control of wound infections using a bilayer chitosan wound dressing with sustainable antibiotic delivery, J. Biomed. Mater. Res. 59 (2002) 438–449.
[85] M. Kong, X.G. Chen, K. Xing, H.J. Park, Antimicrobial properties of chitosan and mode of action: a state of the art review, Int. J. Food Microbiol. 144 (2010) 51–63.
[86] E.I. Rabea, M.E.-T. Badawy, C.V. Stevens, G. Smagghe, W. Steurbaut, Chitosan as antimicrobial agent: applications and mode of action, Biomacromolecules 4 (2003) 1457–1465.
[87] W.A. Sarhan, H.M. Azzazy, I.M. El-Sherbiny, The effect of increasing honey concentration on the properties of the honey/polyvinyl alcohol/chitosan nanofibers, Mater. Sci. Eng., C 67 (2016) 276–284.
[88] P. Koushki, S.H. Bahrami, M. Ranjbar-Mohammadi, Coaxial nanofibers from poly (caprolactone)/poly (vinyl alcohol)/Thyme and their antibacterial properties, J. Ind. Text. 47 (2018) 834–852.
[89] M. Rafiq, T. Hussain, S. Abid, A. Nazir, R. Masood, Development of sodium alginate/PVA antibacterial nanofibers by the incorporation of essential oils, Mater. Res. Exp. 5 (2018) 035007.
[90] I.L. Liakos, A.M. Holban, R. Carzino, S. Lauciello, A.M. Grumezescu, Electrospun fiber pads of cellulose acetate and essential oils with antimicrobial activity, Nanomaterials 7 (2017) 84.
[91] H. Kesici Güler, F. Cengiz Çallıoğlu, E. Sesli Çetin, Antibacterial PVP/cinnamon essential oil nanofibers by emulsion electrospinning, J. Textile Instit. (2018) 1–9.
[92] K. Balasubramanian, K.M. Kodam, Encapsulation of therapeutic lavender oil in an electrolyte assisted polyacrylonitrile nanofibres for antibacterial applications, RSC Adv. 4 (2014) 54892–54901.
[93] W. Zhang, C. Huang, O. Kusmartseva, N.L. Thomas, E. Mele, Electrospinning of polylactic acid fibres containing tea tree and manuka oil, React. Funct. Polym. 117 (2017) 106–111.
[94] S. Baghersad, S.H. Bahrami, M.R. Mohammadi, M.R.M. Mojtahedi, P.B. Milan, Development of biodegradable electrospun gelatin/aloe-vera/poly (ε-caprolactone) hybrid nanofibrous scaffold for application as skin substitutes, Mater. Sci. Eng., C 93 (2018) 367–379.
[95] X. Yang, L. Fan, L. Ma, Y. Wang, S. Lin, F. Yu, X. Pan, G. Luo, D. Zhang, H. Wang, Green electrospun Manuka honey/silk fibroin fibrous matrices as potential wound dressing, Mater. Des. 119 (2017) 76–84.
[96] W.A. Sarhan, H.M. Azzazy, High concentration honey chitosan electrospun nanofibers: biocompatibility and antibacterial effects, Carbohydr. Polym. 122 (2015) 135–143.
[97] N. Charernsriwilaiwat, T. Rojanarata, T. Ngawhirunpat, M. Sukma, P. Opanasopit, Electrospun chitosan-based nanofiber mats loaded with Garcinia mangostana extracts, Int. J. Pharm. 452 (2013) 333–343.
[98] E.J. Lee, B.K. Huh, S.N. Kim, J.Y. Lee, C.G. Park, A.G. Mikos, Y.B. Choy, Application of materials as medical devices with localized drug delivery capabilities for enhanced wound repair, Prog. Mater Sci. 89 (2017) 392–410.
[99] A. Schneider, X. Wang, D. Kaplan, J. Garlick, C. Egles, Biofunctionalized electrospun silk mats as a topical bioactive dressing for accelerated wound healing, Acta Biomater. 5 (2009) 2570–2578.
[100] H. Li, M. Wang, G.R. Williams, J. Wu, X. Sun, Y. Lv, L.-M. Zhu, Electrospun gelatin nanofibers loaded with vitamins A and E as antibacterial wound dressing materials, RSC Adv. 6 (2016) 50267–50277.
[101] H.-J. Lai, C.-H. Kuan, H.-C. Wu, J.-C. Tsai, T.-M. Chen, D.-J. Hsieh, T.-W. Wang, Tailored design of electrospun composite nanofibers with staged release of multiple angiogenic growth factors for chronic wound healing, Acta Biomater. 10 (2014) 4156–4166.
[102] S. Chen, B. Liu, M.A. Carlson, A.F. Gombart, D.A. Reilly, J. Xie, Recent advances in electrospun nanofibers for wound healing, Nanomedicine 12 (2017) 1335–1352.
[103] J. Li, Y.P. Zhang, R.S. Kirsner, Angiogenesis in wound repair: angiogenic growth factors and the extracellular matrix, Microsc. Res. Tech. 60 (2003) 107–114.
[104] H.S. Yang, J. Shin, S.H. Bhang, J.-Y. Shin, J. Park, G.-I. Im, C.-S. Kim, B.-S. Kim, Enhanced skin wound healing by a sustained release of growth factors contained in platelet-rich plasma, Exp. Mol. Med. 43 (2011) 622.
[105] Z. Xie, C.B. Paras, H. Weng, P. Punnakitikashem, L.-C. Su, K. Vu, L. Tang, J. Yang, K.T. Nguyen, Dual growth factor releasing multi-functional nanofibers for wound healing, Acta Biomater. 9 (2013) 9351–9359.
[106] P.D. Pierce, MD, Glenn F, M. Mustoe, Thomas A, Pharmacologic enhancement of wound healing, Annual Review of Medicine, 46 pp. 467–481;1995.
[107] K. Obara, M. Ishihara, T. Ishizuka, M. Fujita, Y. Ozeki, T. Maehara, Y. Saito, H. Yura, T. Matsui, H. Hattori, Photocrosslinkable chitosan hydrogel containing fibroblast growth factor-2 stimulates wound healing in healing-impaired db/db mice, Biomaterials 24 (2003) 3437–3444.
[108] A.A. Ucuzian, A.A. Gassman, A.T. East, H.P. Greisler, Molecular mediators of angiogenesis, J. Burn Care Res. 31 (2010) 158–175.
[109] M. Norouzi, I. Shabani, H.H. Ahvaz, M. Soleimani, PLGA/gelatin hybrid nanofibrous scaffolds encapsulating EGF for skin regeneration, J. Biomed. Mater. Res. Part A 103 (2015) 2225–2235.
[110] M. Piran, S. Vakilian, M. Piran, A. Mohammadi-Sangcheshmeh, S. Hosseinzadeh, A. Ardeshirylajimi, In vitro fibroblast migration by sustained release of PDGF-BB loaded in chitosan nanoparticles incorporated in electrospun nanofibers for wound dressing applications, Artif. Cells Nanomed. Biotechnol. 23 (2018) 1–10.
[111] G. Jin, M.P. Prabhakaran, D. Kai, S. Ramakrishna, Controlled release of multiple epidermal induction factors through core–shell nanofibers for skin regeneration, Eur. J. Pharm. Biopharm. 85 (2013) 689–698.
[112] Z. Wang, Y. Qian, L. Li, L. Pan, L.W. Njunge, L. Dong, L. Yang, Evaluation of emulsion electrospun polycaprolactone/hyaluronan/epidermal growth factor nanofibrous scaffolds for wound healing, J. Biomater. Appl. 30 (2016) 686–698.
[113] J.S. Choi, S.H. Choi, H.S. Yoo, Coaxial electrospun nanofibers for treatment of diabetic ulcers with binary release of multiple growth factors, J. Mater. Chem. 21 (2011) 5258–5267.
[114] P. Zahedi, I. Rezaeian, S.O. Ranaei-Siadat, S.H. Jafari, P. Supaphol, A review on wound dressings with an emphasis on electrospun nanofibrous polymeric bandages, Polym. Adv. Technol. 21 (2010) 77–95.
[115] S.A. Kumar, Wound Healing: Current Understanding and Future Prospect, Int. Journal Drug Discov. 8 (2017) 240–246.
[116] J.K. Stechmiller, Understanding the role of nutrition and wound healing, Nutrit. Clin. Pract. 25 (2010) 61–68.
[117] J. Stechmiller, L. Cowan, K. Logan, Nutrition support for wound healing, Support Line 31 (2009) 61–68.
[118] T. Velnar, T. Bailey, V. Smrkolj, The wound healing process: an overview of the cellular and molecular mechanisms, J. Int. Med. Res. 37 (2009) 1528–1542.
[119] P. Taepaiboon, U. Rungsardthong, P. Supaphol, Vitamin-loaded electrospun cellulose acetate nanofiber mats as transdermal and dermal therapeutic agents of vitamin A acid and vitamin E, Eur. J. Pharm. Biopharm. 67 (2007) 387–397.
[120] X. Sheng, L. Fan, C. He, K. Zhang, X. Mo, H. Wang, Vitamin E-loaded silk fibroin nanofibrous mats fabricated by green process for skin care application, Int. J. Biol. Macromol. 56 (2013) 49–56.
[121] S.A. Kheradvar, J. Nourmohammadi, H. Tabesh, B. Bagheri, Starch nanoparticle as a vitamin E-TPGS carrier loaded in silk fibroin-poly (vinyl alcohol)-Aloe vera nanofibrous dressing, Colloids Surf., B 166 (2018) 9–16.
[122] J. Pullar, A. Carr, M. Vissers, The roles of vitamin C in skin health, Nutrients 9 (2017) 866.
[123] S.A. Guo, L.A. DiPietro, Factors affecting wound healing, J. Dent. Res. 89 (2010) 219–229.
[124] L. Fan, H. Wang, K. Zhang, Z. Cai, C. He, X. Sheng, X. Mo, Vitamin C-reinforcing silk fibroin nanofibrous matrices for skin care application, RSC Adv. 2 (2012) 4110–4119.
[125] M.A. Zarandi, P. Zahedi, I. Rezaeian, A. Salehpour, M. Gholami, B. Motealleh, Drug release, cell adhesion and wound healing evaluations of electrospun carboxymethyl chitosan/polyethylene oxide nanofibres containing phenytoin sodium and vitamin C, IET Nanobiotechnol. 9 (2015) 191–200.
[126] S. Sridhar, J.R. Venugopal, S. Ramakrishna, Improved regeneration potential of fibroblasts using ascorbic acid-blended nanofibrous scaffolds, J. Biomed. Mater. Res. Part A 103 (2015) 3431–3440.

[127] L.I. Moura, A.M. Dias, E. Carvalho, H.C. de Sousa, Recent advances on the development of wound dressings for diabetic foot ulcer treatment—a review, Acta Biomater. 9 (2013) 7093–7114.
[128] P. Beldon, Basic science of wound healing, Surgery (Oxford) 28 (2010) 409–412.
[129] H. Hajiali, M. Summa, D. Russo, A. Armirotti, V. Brunetti, R. Bertorelli, A. Athanassiou, E. Mele, Alginate–lavender nanofibers with antibacterial and anti-inflammatory activity to effectively promote burn healing, J. Mater. Chem. B 4 (2016) 1686–1695.
[130] V. Kant, A. Gopal, N.N. Pathak, P. Kumar, S.K. Tandan, D. Kumar, Antioxidant and anti-inflammatory potential of curcumin accelerated the cutaneous wound healing in streptozotocin-induced diabetic rats, Int. Immunopharmacol. 20 (2014) 322–330.
[131] P.I. Morgado, P.F. Lisboa, M.P. Ribeiro, S.P. Miguel, P.C. Simões, I.J. Correia, A. Aguiar-Ricardo, Poly (vinyl alcohol)/chitosan asymmetrical membranes: Highly controlled morphology toward the ideal wound dressing, J. Membr. Sci. 469 (2014) 262–271.
[132] H.P. Ammon, M.A. Wahl, Pharmacology of *Curcuma longa*, Planta Med. 57 (1991) 1–7.
[133] Y. Abe, S. Hashimoto, T. Horie, Curcumin inhibition of inflammatory cytokine production by human peripheral blood monocytes and alveolar macrophages, Pharmacol. Res. 39 (1999) 41–47.
[134] M.-T. Huang, T. Lysz, T. Ferraro, T.F. Abidi, J.D. Laskin, A.H. Conney, Inhibitory effects of curcumin on in vitro lipoxygenase and cyclooxygenase activities in mouse epidermis, Cancer Res. 51 (1991) 813–819.
[135] J.G. Merrell, S.W. McLaughlin, L. Tie, C.T. Laurencin, A.F. Chen, L.S. Nair, Curcumin-loaded poly (ε-caprolactone) nanofibres: diabetic wound dressing with anti-oxidant and anti-inflammatory properties, Clin. Exp. Pharmacol. Physiol. 36 (2009) 1149–1156.
[136] K. Müller-Decker, W. Hirschner, F. Marks, G. Fürstenberger, The effects of cyclooxygenase isozyme inhibition onincisional wound healing in mouse skin, J. Invest. Dermatol. 119 (2002) 1189–1195.
[137] Y.-J. Park, R. Kwon, Q.Z. Quan, D.H. Oh, J.O. Kim, M.R. Hwang, Y.B. Koo, J.S. Woo, C.S. Yong, H.-G. Choi, Development of novel ibuprofen-loaded solid dispersion with improved bioavailability using aqueous solution, Arch. Pharmacal Res. 32 (2009) 767–772.
[138] B. Steffansen, S.P. Herping, Novel wound models for characterizing ibuprofen release from foam dressings, Int. J. Pharm. 364 (2008) 150–155.
[139] Z. Yuan, J. Zhao, W. Zhu, Z. Yang, B. Li, H. Yang, Q. Zheng, W. Cui, Ibuprofen-loaded electrospun fibrous scaffold doped with sodium bicarbonate for responsively inhibiting inflammation and promoting muscle wound healing in vivo, Biomater. Sci. 2 (2014) 502–511.
[140] M. Mohiti-Asli, S. Saha, S. Murphy, H. Gracz, B. Pourdeyhimi, A. Atala, E. Loboa, Ibuprofen loaded PLA nanofibrous scaffolds increase proliferation of human skin cells in vitro and promote healing of full thickness incision wounds in vivo, J. Biomed. Mater. Res. B Appl. Biomater. 105 (2017) 327–339.
[141] G. Pushpavalli, P. Kalaiarasi, C. Veeramani, K.V. Pugalendi, Effect of chrysin on hepatoprotective and antioxidant status in D-galactosamine-induced hepatitis in rats, Eur. J. Pharmacol. 631 (2010) 36–41.
[142] H. Cho, C.-W. Yun, W.-K. Park, J.-Y. Kong, K.S. Kim, Y. Park, S. Lee, B.-K. Kim, Modulation of the activity of pro-inflammatory enzymes, COX-2 and iNOS, by chrysin derivatives, Pharmacol. Res. 49 (2004) 37–43.
[143] Y. Deldar, Y. Pilehvar-Soltanahmadi, M. Dadashpour, S. Montazer Saheb, M. Rahmati-Yamchi, N. Zarghami, An in vitro examination of the antioxidant, cytoprotective and anti-inflammatory properties of chrysin-loaded nanofibrous mats for potential wound healing applications, Artif. Cells Nanomed. Biotechnol. 46 (2018) 706–716.
[144] A. Basar, S. Castro, S. Torres-Giner, J. Lagaron, H.T. Sasmazel, Novel poly (ε-caprolactone)/gelatin wound dressings prepared by emulsion electrospinning with controlled release capacity of Ketoprofen anti-inflammatory drug, Mater. Sci. Eng., C 81 (2017) 459–468.
[145] I. Romano, M. Summa, J.A. Heredia-Guerrero, R. Spanò, L. Ceseracciu, C. Pignatelli, R. Bertorelli, E. Mele, A. Athanassiou, Fumarate-loaded electrospun nanofibers with anti-inflammatory activity for fast recovery of mild skin burns, Biomed. Mater. 11 (2016) 041001.
[146] Z. Li, H. Kang, N. Che, Z. Liu, P. Li, W. Li, C. Zhang, C. Cao, R. Liu, Y. Huang, Controlled release of liposome-encapsulated Naproxen from core-sheath electrospun nanofibers, Carbohydr. Polym. 111 (2014) 18–24.
[147] J. Varshosaz, A. Jahanian, M. Maktoobian, Montelukast incorporated poly (methyl vinyl ether-co-maleic acid)/poly (lactic-co-glycolic acid) electrospun nanofibers for wound dressing, Fibers Polym. 18 (2017) 2125–2134.
[148] W. Chen, D. Li, A. Ei-Shanshory, M. El-Newehy, H.A. Ei-Hamshary, S.S. Al-Deyab, C. He, X. Mo, Dexamethasone loaded core-shell SF/PEO nanofibers via green electrospinning reduced endothelial cells inflammatory damage, Colloids Surf., B 126 (2015) 561–568.